

LOPES GOMES Paul
Promotion 2015
2015-2016

Diplome d'ingénieur Télécom Physique Strasbourg

Mémoire de stage de 3^{ème} année :

"Photo-detectors development for nEXO"

TRIUMF

4004 Wesbrook Mall V6T 2A3
Vancouver BC Canada
Tel(Fax) 604.222.1047(1074)
www.triumf.ca



RETIERE Fabrice
Tel 604.222.7572
Fax 604.222.1074
fretiere@triumf.ca

Du 2 Mars 2015 au 31 Août 2015

Thanks

First I would like to express my gratitude towards TRIUMF , a national laboratory for particle and nuclear physics, for having welcomed me for those past 25 weeks of internship. I would like to thank especially Mr. Fabrice RETIERE who supervised the work of my team.

Many thanks to Ms. M. MCKAY, head of TRIUMF 's human resources. She helped me to come in Canada and guided me towards TRIUMF during my first days. Many thanks also for Mr. P. LU, Mr. C. CHAMPMAN and Mr. C. LIM for their technical advises about the setup of my internship.

I would like to thank in general each person who made this internship a real academical, professional and human succeed.

Many thanks especially towards my co-workers : Ms. E. TONITA, Mr. C. RETHMEIER and Mr. L. JAMES. I thank also some students from Ottawa's University : Jaqueline, Chriss and Mathiew.

Finally I thank Ms. A.S. CORDAN, Mr. S. LECLER and Mr. J. BAUDOT for their advices and their guidance from the beginning of my internship to my final defense for the master PSA.

Abstract

Founded in 1968 and located on the campus of UBC¹, TRIUMF² is one of the world's leading subatomic physics laboratories. Different research experiments in particle physics are conducted. On the microscopic scale TRIUMF and nEXO³ work together to measure the neutrino-less double beta decay.

¹³⁶Xe may produce such a decay, emitting light at 175 nm. My internship focuses on the characterization of Silicium Photo-Multipliers which will be used to detect this light in the nEXO experiment. To characterize them, efficiency, dark noise, crosstalk and after pulses are calculated at different over-voltages at -100°C.

Results for efficiency are inconsistent because of the initial misalignment of the beam of light coming from a Xenon flash lamp with the surface of photo-detectors. This effect gets worst while the temperature of our setup is cooling down (because of a cooling system). Nevertheless a photo-detector produced by HAMMAMASTU -VUV3 SiPM- shows a dark noise rate less than around 12 Hz/mm² at -100°C and the average number of correlated pulses (crosstalk and after pulses) is less than 0.2 per parent pulses at 5 over-voltage for such a temperature. If the efficiency for such a photo-detector needs to be investigate, previous results show this device as a good candidate for nEXO.

Résumé

Fondé en 1968 et localisé sur le campus de l'UBC, TRIUMF -Laboratoire national Canadien pour la recherche en physique nucléaire et en physique des particules- est l'un des plus importants laboratoires de physique subatomique au monde. Ce laboratoire est à la pointe de la recherche dans plusieurs domaines dont celui de la physique des particules. A l'échelle nanométrique TRIUMF et nEXO travaillent ensemble à la recherche de la désintégration bêta sans 'émission de neutrino.

Si l'élément chimique ¹³⁶Xe est un candidat potentiel pour produire une telle désintégration avec émission de lumière à 175 nm, le but de mon stage est de caractériser des photodétecteurs au silicium (SiPM). De tels détecteurs seront ensuite utilisés par l'expérience nEXO pour capter la lumière (photons) émise. Mesurer l'efficacité quantique de ces détecteurs, le bruit thermique par unité de surface milimétrique, le nombre moyen d'impulsions d'interférence et le nombre moyen de post-implusions ont été effectué -100°C.

Les résultats de l'efficacité quantique ne sont pas reproductibles car le faisceau de la lampe au Xénon n'est pas aligné avec la surface des photodétecteurs. Cet effet s'amplifie au fur et à mesure que la température diminue.

Cependant un photodétecteur de HAMMAMATSU -VUV3 SiPM- présente des propriétés intéressantes pour l'expérience nEXO: le bruit thermique par unité de surface ainsi que le nombre d'impulsions liées à une impulsion primaire (impulsions d'interférence et post-impulsions) sont respectivement moins de 12 Hz/mm² et moins de 0.2 par impulsions primaires pour un excès de tension de 5V. Si l'efficacité quantique doit être étudiée, ce photodétecteur est déjà un bon candidat potentiel pour l'expérience nEXO.

¹University of British Columbia

²Canada's national laboratory for particle and nuclear physics

³next generation Enriched Xenon Observatory

Contents

1	Introduction	1
2	A short abstract about TRIUMF	2
2.1	History and Partners	2
2.1.1	History	2
2.1.2	Partners	3
2.2	Governance and Organization	3
2.3	Research topics at TRIUMF	4
3	Motivations	6
3.1	Understand physical phenomena	6
3.1.1	Is the neutrino a Majorana particle?	7
3.1.2	From EXO-200 to nEXO	8
3.1.3	The subject of my internship	10
4	SiPM Studies	11
4.1	Methodology	11
4.2	The Setup	11
4.2.1	The Xenon flash lamp	12
4.2.2	Photo-detectors and the cooling system	14
4.2.3	Temperature sensors and automation	15
4.3	Silicon Photo-Multiplier	16
4.3.1	Structure	16
4.3.2	Basic operation	17
4.3.3	Physical APD's operation	17
4.3.4	The three main issues of an operating SiPM	20
4.4	Encountered issues	22
4.4.1	Visible light leaks	22
4.4.2	Radiofrequency light leaks	23
4.5	Efficiency of the photo-detectors	25
4.5.1	Methodology used to calculate efficiency	25
4.5.2	Inconsistent results at -100°C	27
4.5.3	Analysis: the misalignment of the light	28
4.6	Dark Noise rate	32
4.6.1	Methodology for dark noise	32
4.6.2	Results	33
4.6.3	Analysis: Poisson distribution	34
4.6.4	conclusion	34
4.7	Correlated avalanches: CT and AP	35

4.7.1	Methodology	35
4.7.2	Results	37
4.7.3	Analysis	39
5	Synthesis	42
6	Professional assessments	43
7	Human impact	44
8	Conclusion	45
A	Terminology	47
B	Details about the setup	48
B.1	Pictures of the setup	48
B.2	Details about waveforms	51
C	Tests	53
C.1	Attenuation of light	53
C.2	Calibration of temperature sensors	54
C.3	Breakdown voltage calculation	55
C.4	Error bars calculation	56
C.4.1	PE	56
C.5	DN	56
C.6	CT	57
C.7	Test to check light leaks	57

List of Figures

2.1	TRIUMF on the globe.	2
2.2	Organisation chart from the Head of TRIUMF to our work team.	4
3.1	Elementary particles according to the <i>Standard model</i> . The leptonic number of the e^- and the ν_e is +1 each while for their own anti-particle is -1 each.	6
3.2	Nuclei with A = 136. Parabola connecting “odd-odd” and “even-even” nuclei are shown. Single β -decay of ^{136}Xe to ^{136}Cs is energetically forbidden.	8
3.3	Scintillation process: the excited atom releases its energy by emitting light (fluorescence photons).	9
3.4	nEXO will increase the resolution of the scintillation energy for the $0\nu\beta\beta$	9
4.1	An aluminum box contains a Xenon flash lamp and two photo-detectors.	12
4.2	Devices to control the Xenon flash lamp	12
4.3	Beam splitter and filters	13
4.4	N2 from that bottle fills the box.	14
4.5	A VUV2 SiPM on the top lets check if the light from the lamp is constant.	14
4.6	A VUV3 SiPM centered on the cooling shock.	15
4.7	Differents SiPM from HAMMAMATSU are tested.	15
4.8	Those devices allow registering temperatures from different parts of the box.	16
4.9	Documentation about SiPM is provided by HAMMAMASTU [5].	17
4.10	A photo-diode shown as a PN junction [8].	18
4.11	A photon triggers an avalanche of electron-hole pairs inside the PN junction.	19
4.12	One pixel of the VUV3 SiPM is fired by photons. Here is the corresponding single pixel avalanche which gives such a pulse shape. Horizontal axis is the time ($1\mu\text{s}/\text{div}$) and Vertical axis is the voltage measured from the photo-detector ($10\text{mv}/\text{div}$).	19
4.13	Dark noise, after-pulse and crosstalk. Horizontal axis is $1\mu\text{s}/\text{div}$ and Vertical axis is $10\text{mv}/\text{div}$	20
4.14	Pulse shapes from a pixel fired by an incoming photon (centered) are exactly the same than pulse shape triggered by hot carriers (left). The blue signal comes from the detector on the top while the yellow one comes from the detector on the bottom. Horizontal axis is $1\mu\text{s}/\text{div}$ and Vertical axis is $20\text{mv}/\text{div}$	20
4.15	After pulses are clearly identified with the persistent mode of the oscilloscope [9].	21
4.16	The incoming photon triggers hot carriers. Then emitted photons may reach a neighboring pixel and trigger there an avalanche [4].	22
4.17	Different solutions to avoid light leaks.	23
4.18	Electronic noise from radio frequency light leaks disturbs signals from the photo-detectors: pulse shapes will be hided or deformed. Horizontal axis is $1\mu\text{s}/\text{div}$ and Vertical axis is $5\text{mv}/\text{div}$	23

4.19	Different technical solutions to clean signals of the photo-detectors from electronic noise.	25
4.20	Dark and light regions.Horizontal axis is $1\mu\text{s}/\text{div}$) and Vertical axis is $10\text{mV}/\text{div}$	26
4.21	Histogram of VUV3 SiPM for an over-voltage of 5V @ -100°C	28
4.22	Inconsistent results for the efficiency of the VUV3 SiPM at -100°C	28
4.23	Hugh variations of the efficiency for the top and bottom after three hours of running.	30
4.24	Effect of the temperature on the position of the two collimators.	31
4.25	The breakdown voltage allows working on the same OV for different temperature and thus to plot DN versus temperature.	33
4.26	Dark noise rate increases with the over-voltage applied on the VUV3 SiPM at -100°C	34
4.27	The shematic algorithm to find after pulses.Pulse shapes are set positive.	36
4.28	An histogram from crosstalk analysis. The device is a VUV3 SiPM at -100°C at 5 over-voltage.	37
4.29	Crosstalk for the VUV3 SiPM reminds below 2 up 6.5 OV.	37
4.30	Those two plots are the unique signature of a photo-detector.	38
4.31	Average Number of after pulses for the VUV3 SiPM at -100°C	38
4.32	Average Number of Correlated Avalanches for the VUV3 SiPM at -100°C	39
B.1	General pictures of the setup.	48
B.2	Different devices used for the setup.	49
B.3	A black box covering the lamp blocks light leaks from it.	49
B.4	Pieces of metal seem to absorbe radio frequency leaks from the lamp.	50
B.5	These two lines on the shock guide to center the photodetector with the hole of 1 mm of the collimator.	50
B.6	It is quiet difficult to align properly the photodetector of the top with a hole of 1 mm.	51
B.7	Increasing the voltage makes appear earlier pulses triggered by photons.	51
B.8	Signals from each photo-detector are increased by using amplifiers.	52
B.9	Electronic saturation from the MEG MPPC.Horizontal axis is $1\mu\text{s}/\text{div}$ and Vertical axis is $1\text{V}/\text{div}$	52
B.10	The blue signal shows photon saturation: too many peaks in the $1.4\mu\text{s}$ region.Horizontal axis is $1\mu\text{s}/\text{div}$ and Vertical axis is $10\text{mV}/\text{div}$	52
C.1	The coefficient of transmission for our filters is less than 20% according to the manufacturer [12].	53
C.2	Temperature of one of the sensors versus temperature displays by the cooling system.	54
C.3	At -80° this figure -gain versus voltage- allow determinate the breakdown voltage thanks to the fitting.	55
C.4	Light leaks from outside of the box.	58

Chapter 1

Introduction

This internship of 25 weeks is the last session of teaching that Télécom Physique Strasbourg offers to its students to complete their engineering studies.

The goal of this internship for the student is to show that he is able to conduct a real engineering or research work. He's also asked to manage a project, to take its responsibilities and to show autonomous at work.

The subject of this internship covers the two main parts of teaching at Télécom Physique Strasbourg . I was asked to have some knowledges both in electronics, waveform processing or coding and also in particle and matter physics. The Master of Subatomics and Astroparticle Physics gave me bases on particles physics and also on physics about detectors.

This report is addressed to next students who will continue our work and also to people interesting in the subject of my internship.

This report will describe first the laboratory TRIUMF and the project on which I have worked. Then I will show the whole work that my team and I did. At least I will conclude and I will give some recommendations for the next students who may continue our work.

At the end of that document some appendixes give more details about precises parts of that research project and allow the reader to go deeper in understanding of the subject.

keywords: Photo-detector, SiPM, efficiency, dark noise rate, after pulses and crosstalk.

Chapter 2

A short abstract about TRIUMF

I worked at TRIUMF from the beginning of April 2015 to the end of August 2015.

2.1 History and Partners

2.1.1 History

TRIUMF is one of the world's leading subatomic physics laboratories and is considered Canada's leading nuclear science research institute. TRIUMF was founded in 1968 by a consortium of four universities whose the University of British Columbia (UBC).The goal was to provide a research needs in particle physics. This laboratory is located on the campus of the University of British Columbia since 1971. It was built around a cyclotron and the first beam of particles was produced in 1974.



Figure 2.1: TRIUMF on the globe.

Over the year TRIUMF has increased its research topics from the early cyclotron ERA (1965-1986) to medical science since 2009. Four main steps reflect current researches conducted at TRIUMF thanks to the accelerator facilities:

- Nuclear Physics,
- Particle Physics,
- Material Sciences

- Medical Sciences.

2.1.2 Partners

As no single university could provide research needs, the initial consortium grows up to 19 different members and associate universities from across Canada. This consortium rules TRIUMF and has allowed it to evolve into a national laboratory.

TRIUMF provides the centralized resources, tools, and expertise for its different Canadian partnerships. These partnerships could be brought together in three different groups:

- Canadian universities partners,
- International partners whose GANIL ¹ (Caen) and ISN (Grenoble) ¹ in France,
- Commercial partners.

2.2 Governance and Organization

Even if TRIUMF is a laboratory, it could be considered like an enterprise that includes on-site technical, engineering , research and administrative staff. Indeed TRIUMF hosts more than 350 scientists, engineers, and staff performing research. Moreover this laboratory attracts over 500 national and international researchers every year and provides advanced research facilities and opportunities to 150 students and postdoctoral fellows each year.

TRIUMF is a mix of material and human resources which allow conducting researches in total autonomous. For example the main parts of our setup are designed and made at TRIUMF .

TRIUMF is organized to optimally meet its objectives while maintaining accountability, quality, and effectiveness. In that way this laboratory is divided in eight different divisions, whose the Science Division.

Science Division is responsible for scheduling experiments approved by the Experimental Evaluation Committee (EEC). This division is also responsible for all components of all systems and subsystems both for all experimental operations at the TRIUMF site and for other infrastructure for external programs whose nEXO.

Dr. Fabrice RETIERE is the head of nEXO experiment :

¹Le Grand Acc'el'erateur National d'Ions Lourds

¹Institut des Sciences Nucléaires

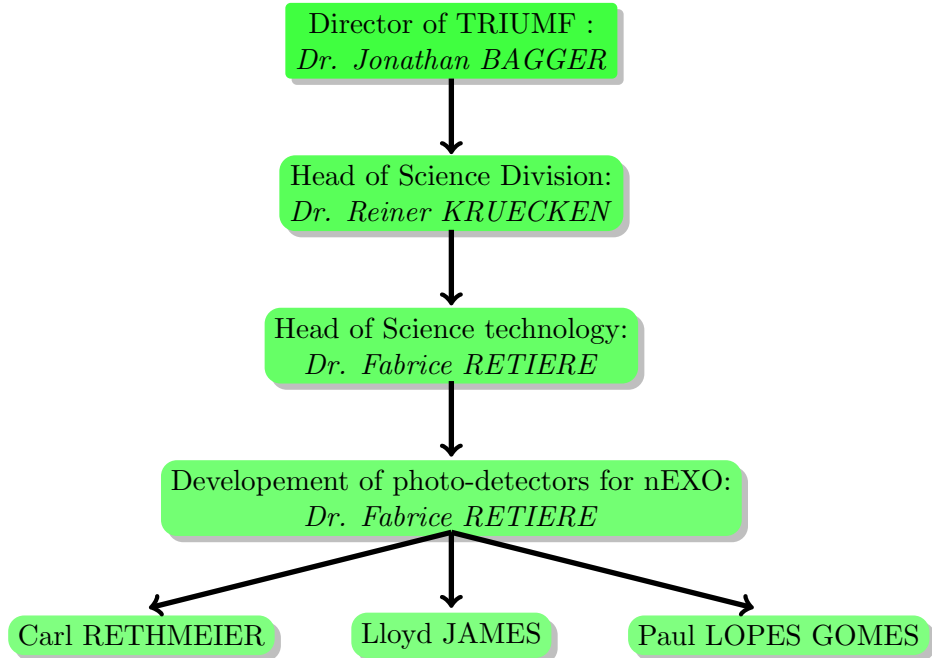


Figure 2.2: Organisation chart from the Head of TRIUMF to our work team.

2.3 Research topics at TRIUMF

As a publicly-funded national laboratory, TRIUMF's activities are framed within its mission and vision with a strategic plan developed every five years. The Government of Canada and other agencies review, approve and finance research experiments.

The strategic plan of TRIUMF could be divided in three main parts :

- The advancing isotopes for science and medicine,
- The harnessing particles and beams for discovery and innovation,
- The understanding of the building blocks of matter and how they shape our universe.

Seven different research topics are conducted at TRIUMF : from nuclear medicine to the investigations in theory group through the particle physics.

These programs exploit the opportunities provided by TRIUMF's core facilities. The driving motivation behind particle physics experiments is the desire to uncover the true nature of fundamental forces and particles. Our current standard model [1] believes to be an effective theory, which has a deeper underlying theory ¹ reachable in the next generation of experiments.

For example in particle physics, in the electroweak sector [1] successes of the past decades have predicted and verified the unification of the electromagnetic and weak nuclear forces. More recently precision measurements at the CERN large electron positron collider (LEP) and the Fermilab proton-antiproton collider (Tevatron) demand that there be either a light Higgs

¹Physics beyond the Standard Model

particle with a mass less than about 200 GeV or a physical system mimicking its interactions.

On the atomic scale (10^{-9}) SNOLAB's experiment focuses on the discovery of neutrinoless double-beta decay which will prove the theory *Physics beyond the Standard Model*.

From SNOLAB to EXO-200

SNOLAB's experiment places it center stage in two quests on opposite scale : on the cosmic scale for interstellar dark matter and on the microscopic scale for neutrinoless double-beta decay.

On the cosmic scale astrophysical measurements indicate that 80% of the matter in the universe is “missing”, which means that this matter does not emit any heat or light. This matter is called dark matter.

Experiments at SNOLAB will search for hypothesized rare interactions between dark matter and normal matter. On the microscopic end of the spectrum, neutrinoless double beta decay probes the very nature of antimatter.

Advanced theories of particle physics and the Big Bang suggest that the neutrino particle may have a special nature: it might be its own antiparticle [3].

Answering this question about the neutrino could give light for future researches on the cosmic scale.

Chapter 3

Motivations

3.1 Understand physical phenomena

Human scale doesn't allow observing what matter is made. But it has been proved theoretically and by experiment that matter is made of elementary particles [1] predicted by the *Standard Model*. The most known elementary particle is the electron. Photon belongs also to that family of elementary particles and it is quiet known that light has the properties of both a wave and a particle, called photon.

The Standard Model divides that family of elementary particles in fundamental fermions and fundamental bosons:

Three Generations of Matter (Fermions)			
	I	II	III
mass →	2.4 MeV/c ²	1.27 GeV/c ²	171.2 GeV/c ²
charge →	2/3	2/3	2/3
spin →	1/2	1/2	1/2
name →	u up	c charm	t top
Quarks	d down	s strange	b bottom
Leptons	v _e electron neutrino	v _μ muon neutrino	v _τ tau neutrino
Gauge Bosons	g gluon	Z ⁰ Z boson	W [±] W boson

Figure 3.1: Elementary particles according to the *Standard model*. The leptonic number of the e^- and ν_e is +1 each while for their own anti-particle is -1 each.

The Standard Model predicts also that antimatter is creating on the same time than matter, which means that there are also antiparticles which have the same mass as particles of ordinary matter but have opposite charge and other particle properties such as the leptonic number 3.1.

Physical properties of particles and antiparticles such mass or energy can be calculated by using certain type of detectors such as mass spectrometers or photo-detectors.

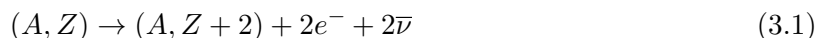
3.1.1 Is the neutrino a Majorana particle?

As it has been reminded above, electronic neutrinos and electronic antineutrinos are particles and antiparticles, respectively.

A currently quest about neutrino is to check if neutrino has a certain characteristic which is to be a Majorana particle ¹. The double beta decay ($2\nu\beta\beta$), predicted by the Standard Model, allows observing such a characteristic.

^{136}Xe is one of the 35 natural isotopes capable of $2\nu\beta\beta$. In such decay a nucleus with charge Z and mass number A ² decays to a nucleus with charge Z+2 and mass number A, where both Z and A are even. We speak about even-even nuclei.

As two neutrons become in two protons, the conservation of the charge implies the creation of two electrons 3.1. As 2 electrons appear, the conservation of the leptonic electronic number implies the creation of two anti-neutrinos 3.2 (The leptonic number for electron and electronic anti-neutrino is given previously):



leptonic electronic conservation :



In case of ^{136}Xe the double beta decay is :



We could observe a single beta-decay instead, if there was not a peculiarity in the nuclear mass function of certain even-even nuclei. This is shown for the case of ^{136}Xe 3.2 where single beta-decay to ^{136}Cs is energetically disfavored over $2\nu\beta\beta$ to $^{136}\text{Ba}^{++}$.

¹In opposition of Dirac particles where particles are distinct from anti-particles.

²The mass number is the total number of nucleons (proton (Z) and neutron (A-Z) within a nucleus

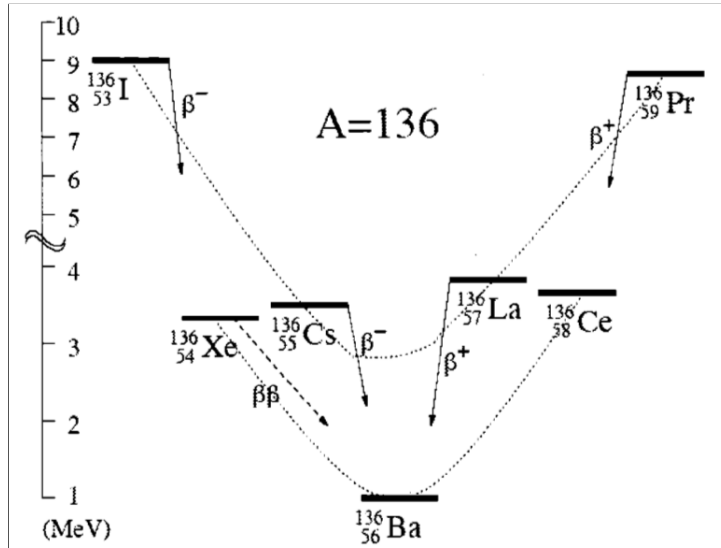


Figure 3.2: Nuclei with $A = 136$. Parabola connecting “odd-odd” and “even-even” nuclei are shown. Single β -decay of ^{136}Xe to ^{136}Cs is energetically forbidden.

Now lets consider the case when neutrinos are Majorana particles which means neutrino and anti-neutrino are identical except for their helicities [1]. If so switching the helicity allows a neutrino to be an anti-neutrino.

That means that the emitted anti-neutrinos is neutrinos which conducts to the equation:



Such a decay releases lots of energy. The energy shares between the nuclei ^{136}Ba and the two electrons. As the mass of the nuclei ^{136}Ba is higher than the one of an electron ³, we could consider, in first approximation, that the ^{136}Ba doesn’t move and that the whole energy is transmitted into kinetic energy to the both electrons.

3.1.2 From EXO-200 to nEXO

EXO-200 is a double beta decay experiment, employing 200 kg of liquid Xe (LXE) in a barrel, isotropically enriched to 80% of ^{136}Xe ⁴.

In such a barrel atoms of ^{136}Xe will decay according to both the double beta decay and the neutrinoless double beta decay (see previous section). From such decays 3.3 the two electrons are ejected with high kinetic energy and scatter off the electrons of other ^{136}Xe atoms.

If so, one of the impacted ^{136}Xe atoms is excited from the ground state and then de-energizes by releasing photons. This is the scintillation process:

³ $\frac{\text{Mass } ^{136}\text{Ba}}{\text{Mass } e^-} = 10^7$

⁴ Neutrons are added to ^{136}Xe atoms. They are told to be in excess of neutrons in oder to observe the beta radioactivity

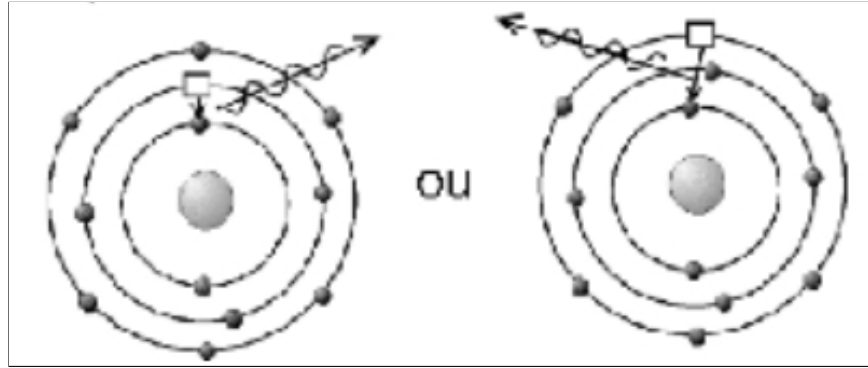


Figure 3.3: Scintillation process: the excited atom releases its energy by emitting light (fluorescence photons).

The scintillation energy of that light comes from $2\nu\beta\beta$ or from $0\nu\beta\beta$ and EXO-200 experiment records this energy by using a type of photo-detector called Avalanche Photo-Diode (APD). The results are plotting in graph showing the scintillation energy versus the ionization energy [4]. The $Q_{\beta\beta}$ shows the $0\nu\beta\beta$ decay:

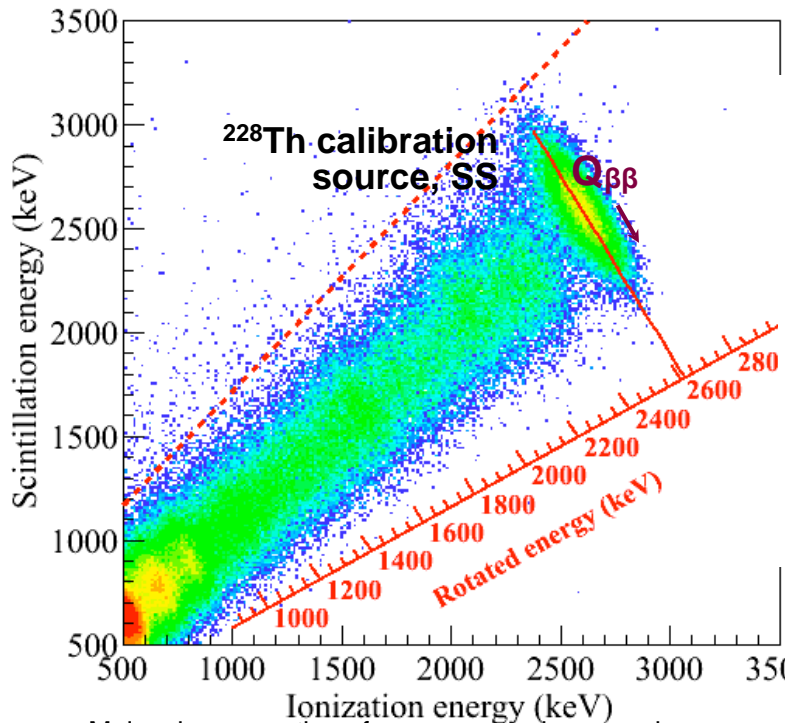


Figure 3.4: nEXO will increase the resolution of the scintillation energy for the $0\nu\beta\beta$.

A simple link between scintillation energy and ionization energy is given in that following equation:

$$E = Q_d + \frac{S_d}{\epsilon}, \quad (3.5)$$

where E , Q_d , S_d and ϵ are the total energy detected, the ionization energy detected, the scintillation energy detected and the efficiency of the APD.

Thus a small variation of the total energy ΔE and the efficiency of the APD ϵ are linked according to that equation:

$$(\Delta E)^2 = \sigma_{Q_d}^2 + \left(\frac{\sqrt{S_d}}{\epsilon} \right)^2 \quad (3.6)$$

Assuming that the scintillation energy detected is linked to the efficiency and to the initial scintillation energy S_i :

$$S_d = S_i \epsilon \quad (3.7)$$

the equation 3.6 becomes:

$$(\Delta E)^2 = \sigma_{Q_d}^2 + \frac{S_i}{\epsilon}. \quad (3.8)$$

From that last equation, we can see that the energy resolution ΔE is inversely proportional to the efficiency of the photo-detectors. The table page 15 of that reference [4] draws a short comparison between two different types of photo-detectors(Avalanche Photo-Diode and Silicium Photo-Multiplier): the efficiency of a SiPM is better than the one of an APD.

The next energy improvement will be to construct the nEXO experiment. This experiment is a collaboration of 19 universities or laboratories whose TRIUMF. nEXO is currently being designed to use 5 tons of enriched liquid Xenon contained in a barrel (instead of 200 kg for EXO-200).

The wall of this barrel will be covered with photo-detector SiPM.

3.1.3 The subject of my internship

The goal of my research internship is to identify suitable SiPMs for nEXO by testing devices from several manufacturers.

In 2014 a test setup was built: a box divided in two parts. The first part contains a Xenon flash lamp which sends photons to the surface of two SiPMs. The signals are observed on the screen of an oscilloscope, which is monitored by a computer. This computer allows registering and storing waveforms. An algorithm (C++ and root) lets us characterize the SiPMs.

The goal is to determine if a selected SiPM could fulfill all the nEXO experiment's requirements:

- Achieve efficiency $\geq 15\%$ at 175nm (the wavelength of Xenon scintillation light),
- Achieve dark noise rate less than 50Hz/mm^2 ,
- Limit the number of correlated pulses (crosstalk and after pulses) to less than 0.2 per parent pulse.

All of those requirements was done at -100°C and in ultraviolet conditions (or VUV) in oder to stay as closer as possible to the operating nEXO experiment (At -100°C and wavelenght of 175 nm).

Chapter 4

SiPM Studies

4.1 Methodology

I worked with 2 others students. We divided the work according to our qualities and skills.

So Carl and I thought about algorithms to analysis waveforms recorded from the oscilloscope. As Carl had yet worked on SiPM before, he wrote mainly different programs to analysis them. Both of us tried to find also technical solutions for different issues we had.

As I worked on the setup the first month of my internship, I was mainly responsible of the setup and of taking data.

As Lloyd worked on the setup one year ago he wrote different programs for the automation stuff. He also wrote a function called “Pulsefinding.exe” to calculate the dark noise and after pulses rate.

Data analysis was made using C++ and ROOT.

This mix of knowledges allows finding technical solutions and thinking about algorithms.

As we were considered as members of the nEXO collaboration we were also able to give regularly talks about the advancement of our work.

4.2 The Setup

The goal is to characterize, at -100°C , photo-detectors receiving light from a xenon flash lamp. In 2014 a setup was built while taking account the two main features of nEXO : working at -100°C and the wavelength of the light from the Xenon flash lamp should be 175 nm.

The picture below 4.1 shows an aluminum box divided into two parts. On the left side is a Xenon flash lamp and on the right side are two photo-detectors.

The photo-detector on the top is used as reference. It allows checking if the light from the lamp reminds constant over time. It also let calculate the absolute efficiency of the photo-detector on the bottom 4.5. The one on the bottom is characterized and a system allows cooling it.

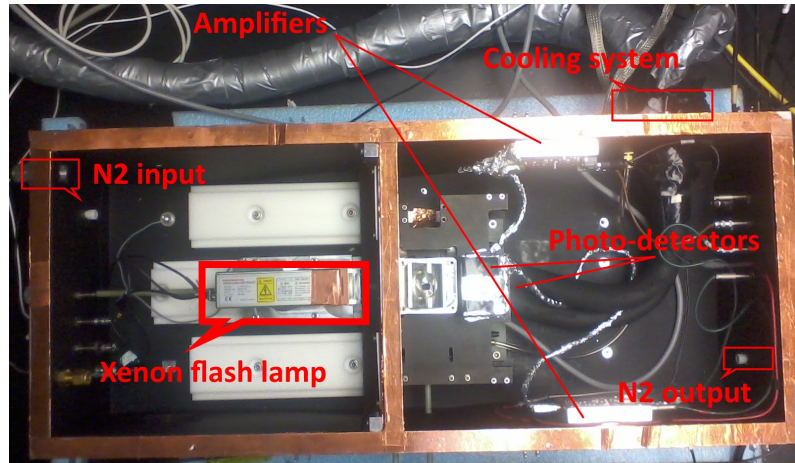


Figure 4.1: An aluminum box contains a Xenon flash lamp and two photo-detectors.

The reader will find more informations and pictures about the setup in the appendix B.

4.2.1 The Xenon flash lamp

A Hamamatsu L11035-03-21 Xenon flash lamp module is used as a light source in a nitrogen-filled, light-tight box to simulate the ultraviolet conditions (VUV) of the future experiment. The amount of light hitting the photo-detectors is managed by a square wave pulse generator, otherwise saturation of the signal from the photo-detectors occurs.

To control light output, and thus the number of photons reaching the photo-detectors, we could move out the lamp away from the area of the detectors since intensity of light drops off as one over distance squared. We could also set the voltage discharge on the lamp by adding an external voltage supply line.

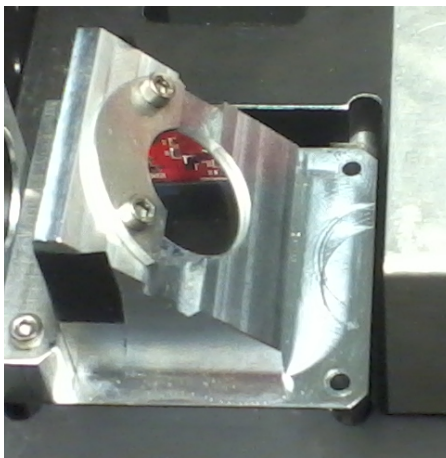


(a) The voltage of the lamp is set by this external supply line.

(b) A pulse generator controls the frequency (10 ms) and the duration of each flash of the lamp ($10\mu s$). The frequency of the lamp is limited by the reading speed of the oscilloscope (20 GHz maxi).

Figure 4.2: Devices to control the Xenon flash lamp

Then the light was collimated by a 5 mm hole, filtered, and then interacts with a beam splitter (BS). The beam splitter separated the incoming beam of 3 mm diameter into two equal beams which reached the surface of each photo-detector on the same time.



(a) The incoming beam reaches the surface of each detectors due to the beam splitter.



(b) The filter in front of the lamp select the VUV region. Both of them attenuate the light of around 20% each.

Figure 4.3: Beam splitter and filters

To select the 175 nm wavelength (VUV region) a filter is added in front of the lamp 4.3(b). A test was made to ensure that no visible light from that lamp could reach the photo-detectors sensitive to the visible wavelength (Otherwise such light could have got wrong our results for the efficiency).

This filter also attenuates the light of the Xenon flash lamp by 20% and that expected attenuation was checked: we found 18.79%. The run is described in the appendix C.

. Then two other identical filters are added before the incoming light reaches the beam splitter (the intensity of the light is too high). We also noticed that the photo-detector on the bottom receives more light than the one on the top. That means that the inclination of the beam splitter is more than 45°. An additional filter is added on the bottom.

As photons of this wavelength have an attenuation length of only a few mm in oxygen, the box was filled with N₂ gas. The second advantage of using N₂ is to avoid frost on the surface of the cooling photo-detectors on the bottom.

Also the appendix B or informations provided by HAMMAMATSU [6] gives the pulse shape of the lamp. We can notice that the pulse shape last around 140 ns and the relative light output reaches 100% after 400 ns. The time of 1.4 μ s is seen on the screen of the oscilloscope C.



Figure 4.4: N₂ from that bottle fills the box.

4.2.2 Photo-detectors and the cooling system

Two photo-detectors were used for each run to calculate the efficiency.

The one on the top allow ensuring that the light remains constant over the time. For that we used a VUV2 SiPM from HAMMAMATSU.

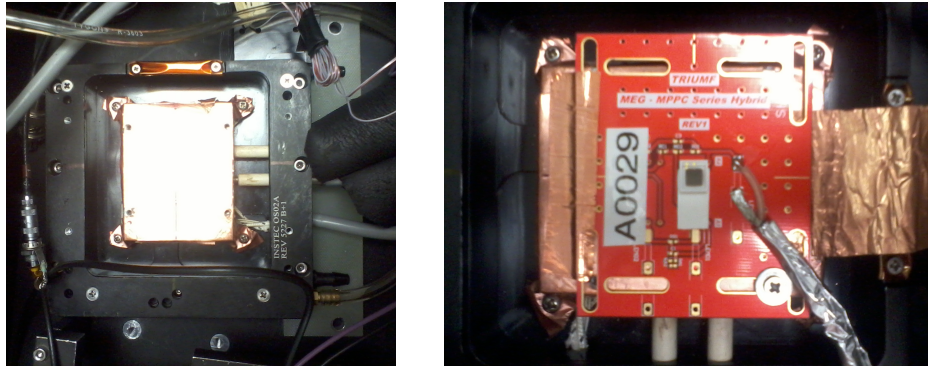


Figure 4.5: A VUV2 SiPM on the top lets check if the light from the lamp is constant.

We chose such a detector because the dark noise rate 4.6 is quite low at room temperature (20°C). So it is possible to calculate the relative efficiency of that detector at such temperature.

The photo-detector on the bottom were characterized (calculate the efficiency at -100°C , the dark noise rate and the number of correlated pulses).

A cooling system allows working at such a low temperature and the photo-detector to characterize was laying on a shock. A plastic board with low thermal conductivity holds the whole cooling shock to avoid thermal leaks.



(a) The cooling system lets work up to -110°C .
(b) VUV3 SiPM of HAMMAMATSU centered on the shock.

Figure 4.6: A VUV3 SiPM centered on the cooling shock.

Several different SiPMs are tested to select the more suitable one for nEXO.

SiPMs from HAMMAMATSU				
	Efficiency	Dark Noise rate	Cross Talk	After Pulse
MPPC MEG	no	yes	yes	no
VUV3 SiPM	no	yes	yes	yes
Coated SiPM	no	yes	yes	no

Figure 4.7: Differents SiPM from HAMMAMATSU are tested.

4.2.3 Temperature sensors and automation

We noticed that the whole box is cooling down over time when we are working at -100°C . The plastic holder of the figure 4.6(a) doesn't isolate totally the colling shock from the rest the box. To check if the decreasing temperature of the box could have an impact on our results (efficiency), 10 temperature sensors are installed inside the box after calibrating them C. All temperatures of the sensors are recorded automatically.



(a) One of the ten temperature sensors.



(b) That device lets record temperatures from sensors.

Figure 4.8: Those devices allow registering temperatures from different parts of the box.

Also a program is written to set the voltage, to record both the current of the photo-detectors and temperatures from different parts of the box.

4.3 Silicon Photo-Multiplier

A Silicon photomultiplier (SiPM) is an electronic device used to detect light (photon). Many groups study their applicability in many different fields such as high-energy, physics calorimetry, astrophysics or medical imaging.

Compared to EXO experiment which uses currently APD, SiPMs for nEXO experiment are a very promising alternative because of the very good properties of such devices:

- SiPMs are incentive to magnetic fields,
- SiPMs' operation voltage is very low,
- SiPMs' gain is $10^6 - 10^7$,
- SiPMs have a very good time (ns) and photon-counting resolutions (μm) due to the size of one pixel.

4.3.1 Structure

This device consists a matrix of typically 1000 independent and equal micro-cells (pixels) per mm^2 . A pixel consists the basic element of SiPMs.

Each pixel are connected in parallel. They are formed out of an Avalanche Photo Diode (APD) and a quenching resistor which is connected in series to an APD.

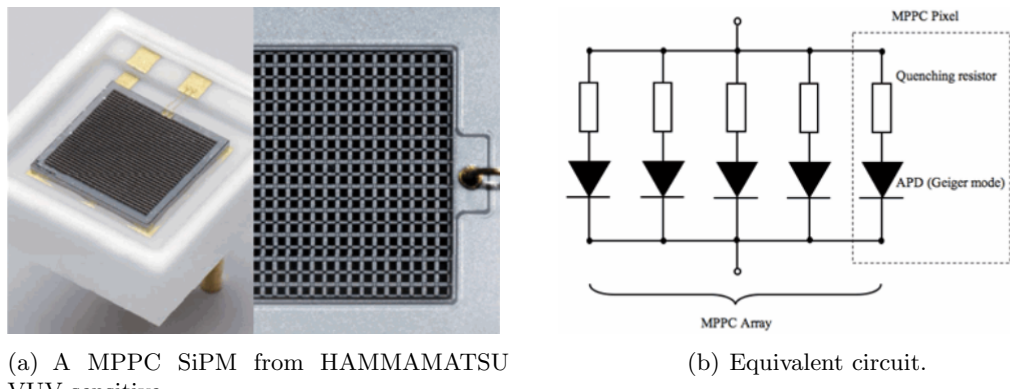


Figure 4.9: Documentation about SiPM is provided by HAMMAMASTU [5].

The appendix B gives more details about the amplification of signals from photo-detectors.

4.3.2 Basic operation

Each pixel in a SiPM outputs a pulse at the same amplitude when it detects a photon. A pulse produced from one pixel doesn't vary with the number of incident photons firing that pixel. All pixels are connected to the same output channel. The total output signal is equal to the sum of those from the individual pixels firing by photons.

For example, if four photons are incident on different pixels and detected at the same time, then the SiPM outputs a signal whose amplitude equals the height of the four superimposed pulses.

One feature of an SiPM is that each APDs operate in Geiger mode.

4.3.3 Physical APD's operation

PN Junction

A pixel is a photo-diode and a photo-diode has the structure of a PN junction. This reference [7] could remind the reader how a PN junction works:

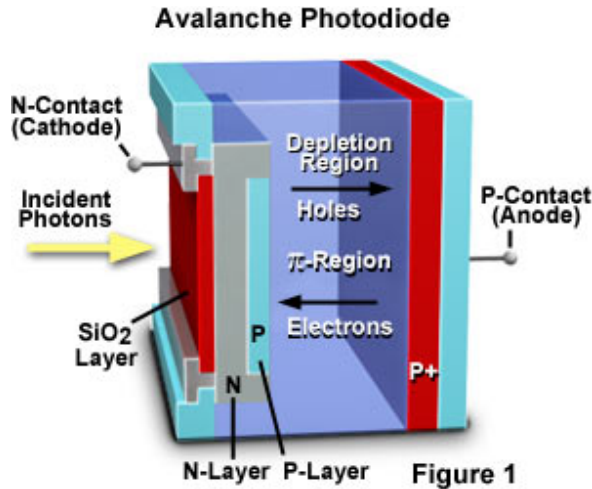


Figure 4.10: A photo-diode shown as a PN junction [8].

Principle of avalanche multiplication

The principle of an APD is based on the conversion of the energy of photon into free charge carriers (electrons and holes) in the depletion region and their further multiplication via the process of the impact ionization.

When light (photon) enters a photo-diode, electron-hole pairs are generated if the light energy is higher than the band gap energy. Light energy - E_{light} in electron-volt (ev)- and wavelength λ (nm) are in relationship as shown in equation (number) below.

$$E_{light} = \frac{123}{\lambda} \quad (4.1)$$

A reverse voltage (or bias voltage) is applied to each opposite sides (cathode and anode) of a PN junction. The reverse voltage applied on an PN junction is upper than the Breakdown Voltage (BV) of that APD: this is the Geiger mode ¹.

The reversed (or biased) voltage V_{biased} and the breakdown voltage $V_{breakdown}$ are linked with the over-voltage (OV or ΔV) according to that relation :

$$\Delta V = V_{biased} - V_{breakdown} \quad (4.2)$$

Also this reverse voltage creates an electric field developed across the PN junction. When an electron-hole pair is generated in the depletion layer of a photo-diode the electrons (negative charge) drift towards the N layer (where the cathode is) while the holes drift towards the P+ layer (where the anode stays). This migration is due to the electric field.

The drift speed of these electron-hole pairs or carriers depends on the electric field strength. To a certain speed the carriers collide with the atoms (called crystal lattice) of the structure. If the reverse voltage is increasing even further, some of the carriers which escaped primary collision with the crystal lattice will have a great energy.

¹Conventional photo-diodes operate in linear mode

When they collide later with the crystal lattice, they will generate other electron-hole pairs. This physical phenomena is called ionization: an electron or a hole with high kinetic energy ionizes the matter by triggering other electron-hole pairs. By the end an avalanche phenomena is observed inside the avalanche region of a PN junction:

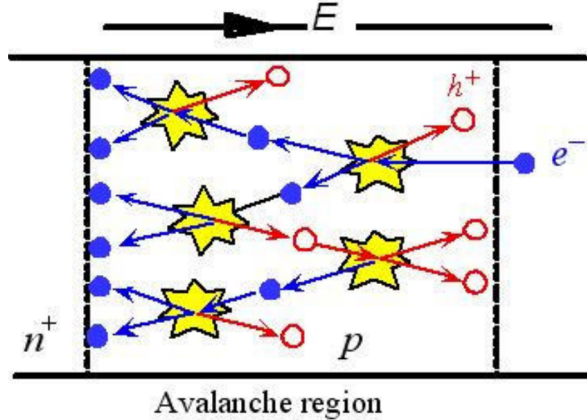


Figure 4.11: A photon triggers an avalanche of electron-hole pairs inside the PN junction.

The electrons of that avalanche phenomena are collected on the cathode. The resulting current is used to plot the pulse shape. To control an avalanche and so the corresponding current, a resistor is set in series with an PN junction ². When the avalanche current flows through the resistor, the bias voltage applied to the junction drops below the breakdown voltage. This quenches the avalanche; thus, the current decreases to zero, and the reverse voltage across the PN junction increases again above its BV.

Then the pixel is ready to detect the arrival of a new photon.

A single pixel avalanche gives a pulse shape observed on the screen of an oscilloscope:

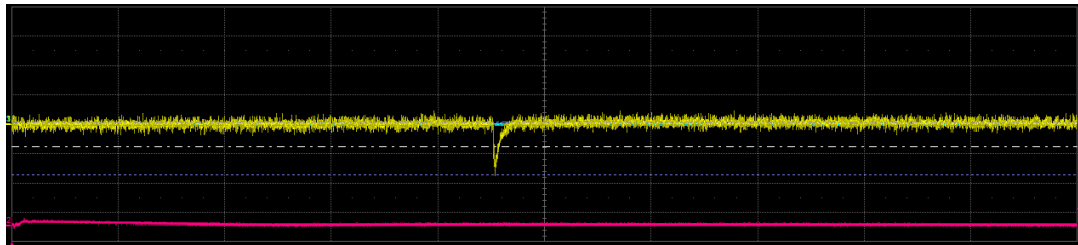


Figure 4.12: One pixel of the VUV3 SiPM is fired by photons. Here is the corresponding single pixel avalanche which gives such a pulse shape. Horizontal axis is the time ($1\mu s/\text{div}$) and Vertical axis is the voltage measured from the photo-detector ($10\text{mV}/\text{div}$).

²The avalanche is also limited by the buildup of a limiting space charge in the depletion region which makes decrease the field.

4.3.4 The three main issues of an operating SiPM

Such an ideal picture is strongly modified by the occurrence of phenomena leading to dark current, after-pulsing effects and crosstalk:

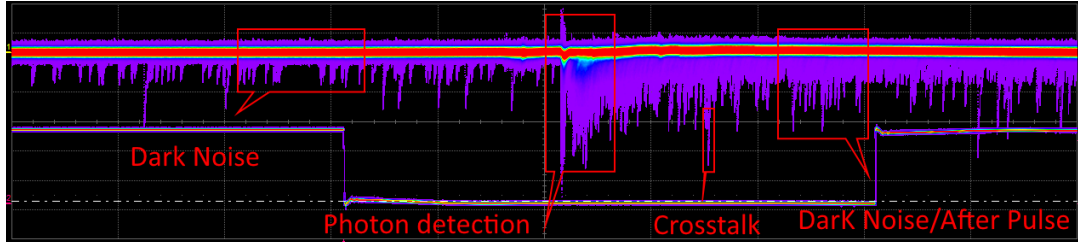


Figure 4.13: Dark noise, after-pulse and crosstalk. Horizontal axis is $1\mu\text{s}/\text{div}$ and Vertical axis is $10\text{mv}/\text{div}$.

Dark Noise

One of the main source of noise limiting APDs' performance is the dark noise rate. Electron-hole pairs are generated thermally in the depletion region. Due to the reversed bias voltage applied on the PN junction, the avalanche phenomena occurs. Unfortunately it is not possible to make the difference between avalanche triggered by a photon and avalanche triggered by hot carriers. The figure below shows that evidence:

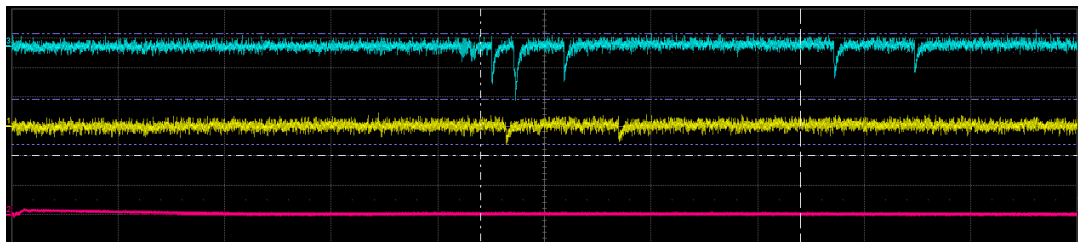


Figure 4.14: Pulse shapes from a pixel fired by an incoming photon (centered) are exactly the same than pulse shape triggered by hot carriers (left). The blue signal comes from the detector on the top while the yellow one comes from the detector on the bottom. Horizontal axis is $1\mu\text{s}/\text{div}$ and Vertical axis is $20\text{mv}/\text{div}$.

Dark noise depends only of the structure of the SiPM. VUV3 SiPM from HAMMAMASTU has a lower dark noise rate than VUV2 or MPPC MEG from the same manufacturer. Nevertheless it is possible to decrease the dark noise rate by cooling down the SiPM since dark noise is generated by hot carriers.

Crosstalk and after-pulses are generated by primary peaks. By definition a primary peak can be triggered by photon or by hot carriers.

Trapping phenomena: Afterpulsing

Traps may result from damage caused by an implantation of some impurities in the fabrication process. In the depletion region, deep levels trap some avalanche carriers and release them with a statistical delay. If the delay is greater than the dead time after the previous avalanche pulse, a released carrier can re-trigger an avalanche and cause a statistically correlated pulse. These delayed correlated pulses are known as after pulses.

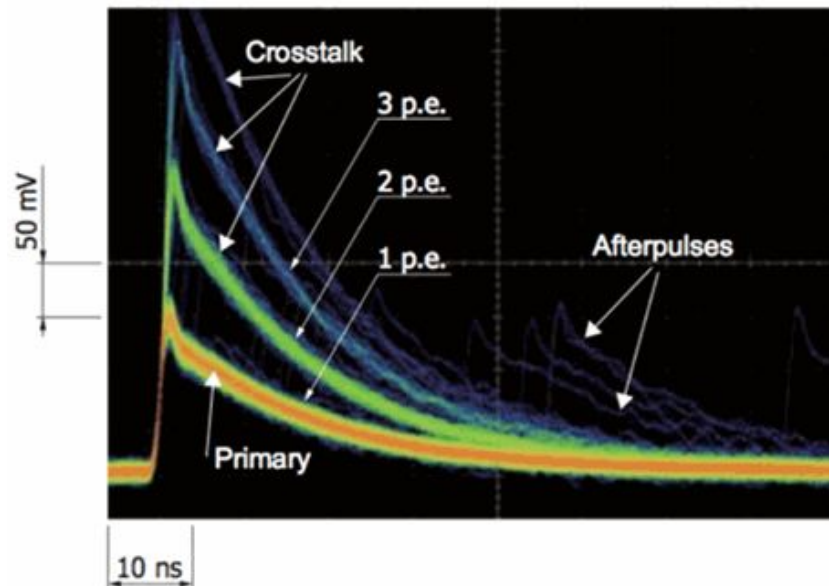


Figure 4.15: After pulses are clearly identified with the persistent mode of the oscilloscope [9].

The probability that an after pulse occurs increases with the reversed bias voltage applied on the SiPM. A solution to diminish significantly after pulses effects is to operate at low reversed bias voltage, but at the expense of degrading the photon-detection efficiency 4.5.

Optical crosstalk

In the P+ layer of a PN junction, hot carriers (e.g., dark noise) of an avalanche has a certain probability to emit photons with energy higher than 1.14 eV (higher than the band gap energy of the silicon (1.12 eV)).

Depending on their energy and the location where they are produced, these photons have a certain probability to reach a neighboring pixel and to produce an additional avalanche.

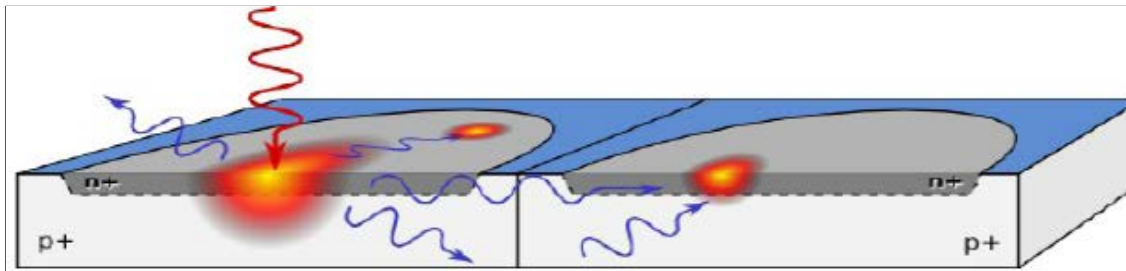


Figure 4.16: The incoming **photon** triggers hot carriers. Then emitted **photons** may reach a neighboring pixel and trigger there an avalanche [4].

When several pixels are fired by an incoming photons or by photons created in the P+ layer, the high of the resulting pulse shape “is multiplied” by the number of fired pixels³.

A technical solution is to build an optical wall between two pixels not to let created photons reaching neighboring pixels. The same conclusion about the efficiency for after-pulses can be made for crosstalk.

4.4 Encountered issues

Before recording waveforms and analyzing them I encountered with some issues but mainly with electronic noise.

Light leaks appeared when the Xenon flash lamp is operating. They can hinder and negate the results of data collection. Two kinds of light leaks have been observed :

- Visible light leaks.
- Radiofrequency light leaks.

4.4.1 Visible light leaks

Visible light leaks come from outside of the box or from the Xenon flash lamp (visible light leak).

This phenomena has mainly an impact on the dark noise rate and on the calculation of the efficiency. To avoid visible light from the Xenon flash lamp , the lamp is covered with a black box. Also to absorb photons from such visible light walls and lid are covered by matt black absorbing vin.

To avoid light from outside of the box, the whole box was covered with a black tissue. The section C shows how we checked if some visible light from outside could reach detectors inside the box.

³The section 4.3.2 reminds that “The total output signal is equal to the sum of those from the individual pixels firing by photons”.



(a) A black tissue lets avoid light from outside the box.

(b) Black vin, covering the wall and the bottom of the box, absorbs light leaks from the Xenon flash lamp .

Figure 4.17: Different solutions to avoid light leaks.

4.4.2 Radiofrequency light leaks

Radio frequency light leaks result in electromagnetic noise on the signals from the detectors. Radio frequency noise occurred when the Xenon flash lamp is triggered (by a square wave pulse generator). Too much radio frequency noise disturbs the signals of the photo-detectors. This figure below shows clearly that electronic noise covers, deforms or amplifies pulse shapes.

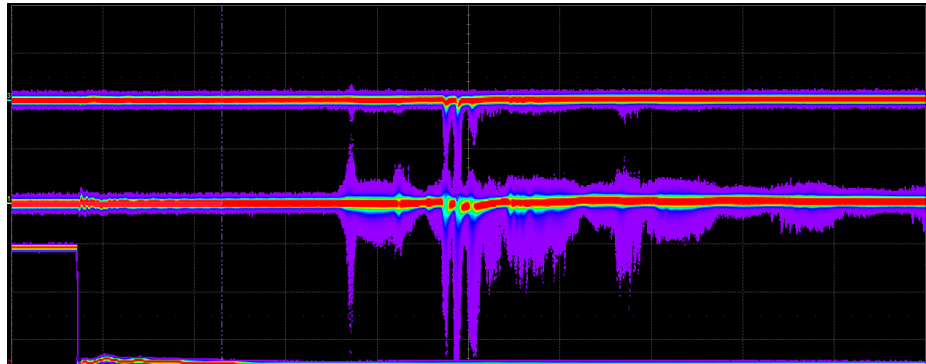


Figure 4.18: Electronic noise from radio frequency light leaks disturbs signals from the photo-detectors: pulse shapes will be hided or deformed. Horizontal axis is $1\mu\text{s}/\text{div}$ and Vertical axis is $5\text{mV}/\text{div}$.

Sources of electromagnetic noise

We have noticed that electronic noise comes from electromagnetic sources:

- Some devices were not grounded. The signal from the photo-detectors oscillates 4.18
- When the Xenon flash lamp is working it is creating some radio waves which propagate through the air and are then transmitted to any piece of conductive metal of the box. The consequences are :

- The aluminum lid of the box conducts everywhere the electric field of these radio waves, which disturb the amplifiers.
- Each detector could feel these radio waves and the signal got worst.
- The metal divider acts as a transmitter and the piece of metal of the signal wires connected to the amplifiers acts as antenna.

Three main solutions

The first solution is to create a ground point on which all devices - especially the square wave pulse generator - are connected with the same wire (to avoid ground loops). In that way, the oscillations of 4.18 are removed.

Isolate the lid from the box As it is described above, the electric field from the radio waves propagates through the entire lid. When the box is closed the electric field disturbs the operating amplifiers. The solution is to isolate the lid from the box by adding black tape and, to guide the electric field, by adding copper on the edge of the lid to the ground point.

Isolate the Xenon flash lamp As the Xenon flash lamp creates radio waves, we decided to isolate it by building a Faraday cage around it. We added a thick piece of metal to absorb radio waves and we covered this first part of the box with aluminum foil. In that way the electric field propagates through the aluminum foil to the edge of the top box to the ground point.

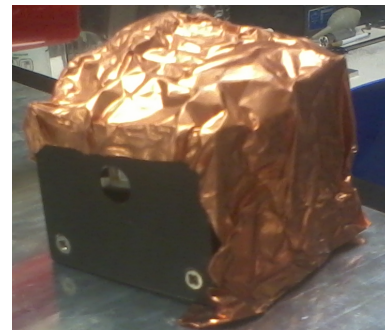
Isolate the photo-detectors and the amplifiers The wire which connects a photo-detector to an amplifier seems to act like an antenna and transmits radio waves. A solution has been to enroll such a wire with aluminum foil. The amplifier and the ground of the photo-detector are connected due to the aluminum foil.

Another solution is to isolate the photo-detectors on the top and on the bottom by building Faraday cage around them.

Those pictures below could summarize our work (yellow signal is the photo-detector on the bottom while the blue one is from the photo-detector on the top):



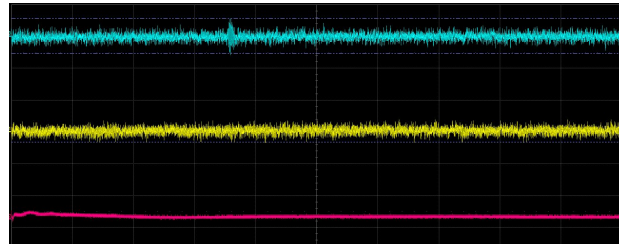
(a) A thin copper foil allows good contact between the lid and the top of the box.



(b) A Faraday cage around each photo-detector isolates them from radio frequency leaks.



(c) Each signal wire is enrobed with aluminum foil touching the ground part of each photo-detector.



(d) Without electronic noise pulse shapes can be identified from Gaussian noise. Horizontal axis is $1\mu\text{s}/\text{div}$ and Vertical axis is the amplitude ($5\text{mV}/\text{div}$).

Figure 4.19: Different technical solutions to clean signals of the photo-detectors from electronic noise.

A SiPM, placed on the top, is used as a reference. It let us check if the light reminds constant when we characterize a MEG MPPC or a VUV3 SiPM at -100°C .

4.5 Efficiency of the photo-detectors

Measuring the efficiency of the SiPM is one of the most important test to characterize them. A paper from nEXO [10] and another one [11] described how to measure the efficiency of SiPMs but not in our working experimental conditions: the wavelength of light is 175 nm and the efficiency has been calculated at -100°C .

4.5.1 Methodology used to calculate efficiency

Theoretical calculation

The previous paper from nEXO [10] allows calculating the theoretical efficiency.

A simple way to calculate the efficiency is to define two regions in the scope: the “dark region” is the time before the Xenon flash lamp triggers and the “light region” is the time immediately after the flash lamp triggers. So pulse shapes triggered by photons can only appear on the light region.

The both regions has the same size - $3\mu\text{s}$ ⁴ each - to allow comparing those two regions. The section 4.3.4 reminds that pulses triggered by photons or by hot carriers (dark noise) have the same shape. Moreover pulse shapes from dark noise can appear anywhere in those two regions:

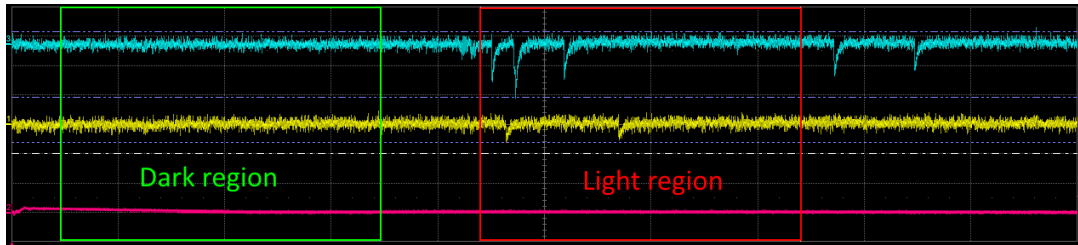


Figure 4.20: Dark and light regions. Horizontal axis is $1\mu\text{s}/\text{div}$) and Vertical axis is $10\text{mv}/\text{div}$.

The average number of Photon Electron (which is the efficiency) - $\langle PE \rangle$ - of a photo-detector is defined with this relation below:

The probability of observing zero photon in the "light region" is :

$$P_{L0} = \frac{N_{L0}}{N_{tot}}, \quad (4.3)$$

The probability of observing zero photon in the "dark region" is :

$$P_{D0} = \frac{N_{D0}}{N_{tot}}, \quad (4.4)$$

where N_{L0} is the number of times of not observing any pulses in the "light region" and N_{D0} is the number of time of not observing any pules in the "dark region". N_{tot} is the total number of events.

The probability of obtaining zero dark noise P_{DN0} and the probability of obtaining zero photo electron from the lamp P_{Lamp0} follow a Poisson distribution. These two probabilities are linked by the probability P_{L0} :

$$P_{L0} = P_{Lamp0} \cdot P_{DN0}, \text{ where } P_{Lamp0} = e^{-\langle PE \rangle} \text{ and } P_{DN0} = e^{-DN} \quad (4.5)$$

$$\text{So : } e^{-\langle PE \rangle} = \frac{P_{L0}}{P_{D0}} \quad (4.6)$$

$$\langle PE \rangle = -\ln\left(\frac{P_{L0}}{P_{D0}}\right). \quad (4.7)$$

Setting and analysis

On the scope we trigger on the lamp. The scope displays a waveform on $10\mu\text{s}$ since the Xenon flash lamp is on during $10\mu\text{s}$ (with a frequency of 100Hz)

During this lapse of time, we noticed that the lamp needs more than $4\mu\text{s}$ before sending photons.

⁴Time base is $1\mu\text{s}/\text{div}$

After $4\mu s$ we could noticed pulse shapes triggered by photons.

Also as it is shown on these screen-shots of the oscilloscope C the voltage set on the lamp influence the position in time of pulse shapes triggered by photons. Moreover the pulse shape of the lamp B lasts around $1.4\mu s$ which means that most of such pulse shapes will appear in that lapse of time C. So the size of the "light and dark region" could have been set at around $1.4\mu s$. For example, with a window size of $3\mu s$, the dark region begins at $0.9\mu s$ and end at $3.9\mu s$ while the light region begins at $5\mu s$ and end at $8\mu s$.

The oscilloscope is monitored and it is possible to record, on the same time, a predefined number of waveform (we choose 15000 waveforms).

The C++ code "efficiency.exe" smooths a waveform (to decrease the Gaussian noise and increase the ratio Signal/Noise), records the minimum of it in each regions and plots an histogram which allows counting the number of zero photon electron (0PE) in the "light and dark region".

Here is an example of line command: `bin/efficiency.exe -r 1733 -s 10 -w 3000 -b 900 -a 5000`, with "-r" is for the number of the *run*, "-s" to set the *smoothing*, "-b" to set the beginning of the "dark region", *before* pulses triggered by photons and "-a" to set the beginning of the "light region", *after* pulses triggered by photons.

4.5.2 Inconsistent results at -100°C

Here is one of our results for the VUV3 SiPM at -100°C with an over-voltage of 5V (At such temperature the breakdown voltage is 44.73V). The appendix C could explain how to calculate the breakdown voltage for each device at different temperatures.

The histogram below shows from right to left zero photon electron (0PE), one photon electron (1PE):

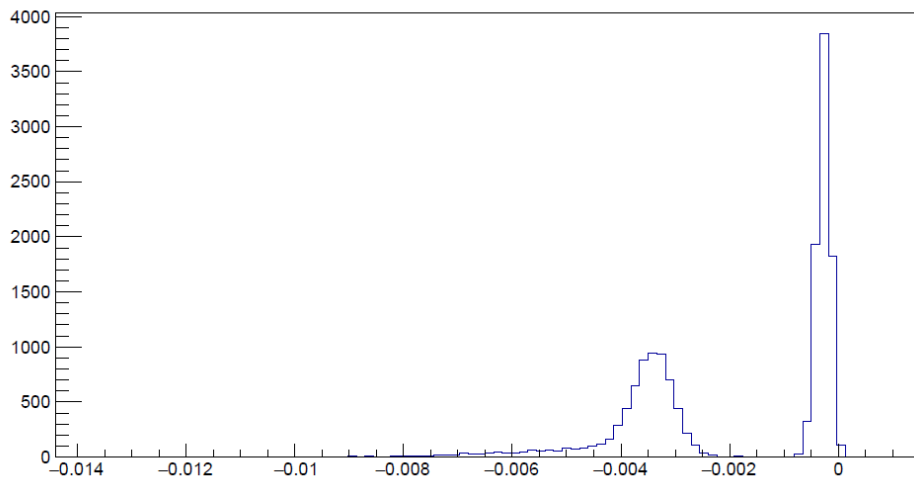


Figure 4.21: Histogram of VUV3 SiPM for an over-voltage of 5V @ -100°C .

Several tests on the same experimental conditions are made to see if our results for the VUV3 SiPM are reproducible:

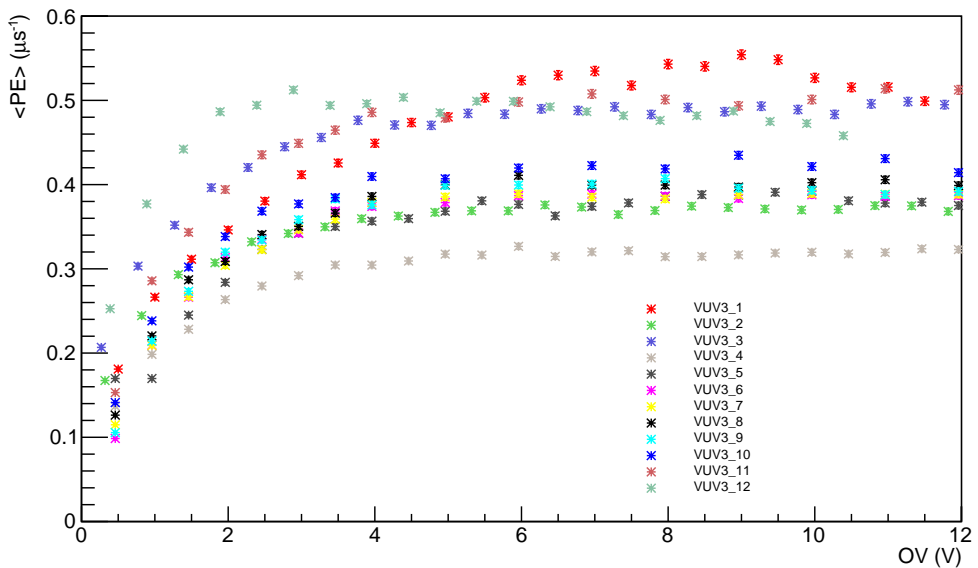


Figure 4.22: Inconsistent results for the efficiency of the VUV3 SiPM at -100°C .

The error bars are quiet small (the appendix C details the error bars calculation.)

4.5.3 Analysis: the misalignment of the light

We would like to count the number of time we see a pulse corresponding to 1PE peak. 1PE peak can come from a single pixel avalanches triggered by photons or from avalanches triggered by hot carriers (dark noise).

Moreover in the light region it is not possible to make the difference between a pulse shape triggered by a photon or by hot carriers. One solution is to take in account pulse shapes from dark noise in the "dark region". In that region we know for sure that 1PE peak comes obviously

from dark noise.

Considering the fact that dark noise in the light region or in the dark region appears at the same rate 4.5, a solution will be to divided the 0PE peak of the "light region" by the 0PE peak from the dark region.

The function -ln- comes from the Poisson distribution.

Whatever is the run the efficiency increases as ln function. Moreover when we increase the reversed voltage of a photo-detector, the probability of observing crosstalk increases (so the 2 PE peak increases) and thus the probability of observing 0PE peak decreases for a same number of waveforms. So the number 0PE peak from the "light region" decreases faster than the one from the "dark region", which explains those ln variations.

Nevertheless such observations don't explain such an inconsistency of the efficiency at -100°C . We made those different runs with the same VUV3 SiPM. So at the same temperature, the breakdown voltage is the same. Five parameters could explain such an inconsistency:

- The voltage of the lamp,
- The quantity of oxygen inside the box,
- Dust on the area of the photo-detectors,
- The size of the screen of the oscilloscope,
- The alignment of the photo-detectors with the beam of light.

The fourth first parameters

The voltage of the lamp has two impacts on the efficiency.

First when the voltage is increasing the Xenon flash lamp sends more light and so more photons trigger avalanches inside an SiPM. According to the previous section, the efficiency decreases. Second as explained previously the voltage of the lamp influence the position in time of pulse shapes triggered by photons.

So if the voltage of the lamp changes between each run, the "light and dark region" will change also and so the efficiency will change for a same over voltage of a photo-detector.

Nevertheless we set the voltage of the lamp at 2.8V for each run. The setting for the "light and drak region" is described above.

The quantity of oxygen inside the box could have an impact on the efficiency. The box is filled with N₂ to allow propagation of photons from the lamp to the detectors. It also lets avoid frost on the area of the photo-detectors cooled on the bottom of the box. So far no frost has been observed but the quantity of oxygen inside the box has not been checked.

On the contrary we have already seen some dust on the area the photo-detectors. Run 2 and run 3 4.22 show that reality. During the run 2 some dust was on the area of the photo-detector on the bottom while dust was blowed out for the next run (run 3).

The windows size of the screen of the oscilloscope has an influence on the efficiency. Indeed

the increasing voltage applied on the photo-detectors increases the height of any pulse shapes. At low voltage all pulse shapes (especially crosstalk since pulses from crosstalk are at least twice higher than pulse shape from single pixel avalanches) are not cut by the windows size (5mV/div). At high voltage all pulse shapes are cut by such a small window size and thus histograms will not let make the difference between 0PE, 1PE, 2PE ...

That is why the windows size needs to be adjust when the voltage of the photo-detectors changes.

Effect of the temperature

To check if the efficiency of the two photo-detectors remains constant over the time at -100°C , four run are made. We have also noticed that the beam splitter seems to move at such low temperature (which means that temperature seems to have an impact on the beam splitter). For that here are the parameters we changed between different runs:

- run 1: @ -100°C , with beam splitter,
- run 2: @ -100°C , without beam splitter,
- run 3: @ RT, with beam splitter,
- run 4: @ RT, without beam splitter.

The other parameters remain the same between different runs : the over-voltage and the position of the photo-detectors⁵, the voltage and the position of the lamp, the box filled with N2 and the stabilization of the temperature at -100°C (wait at least 30 min for that).

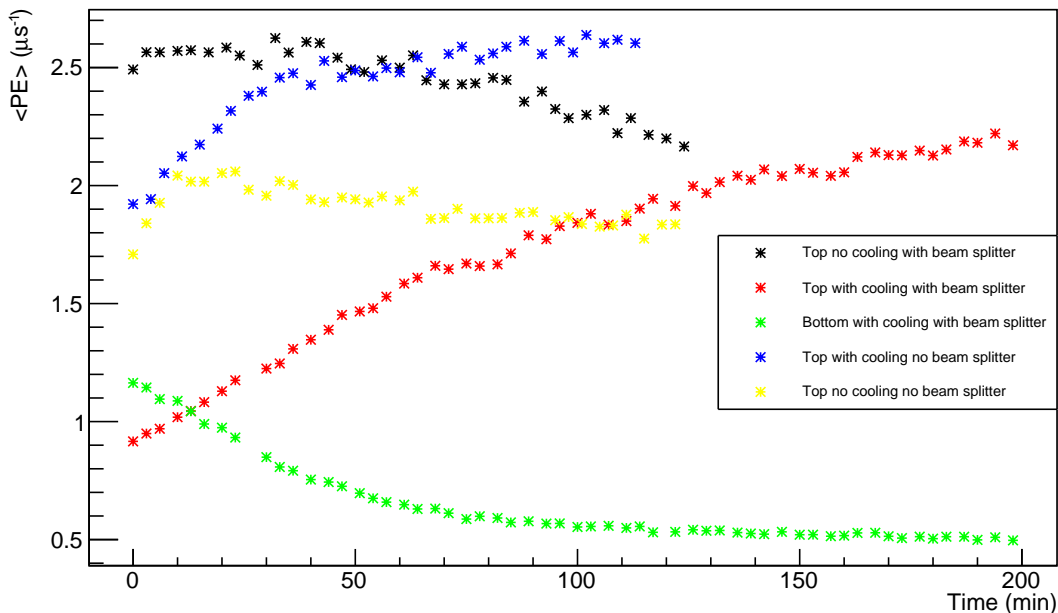


Figure 4.23: Hugh variations of the efficiency for the top and bottom after three hours of running.

⁵For the bottom one, the over-voltage is different at RT than at -100°C since the breakdown voltage decreases with temperature C

So far the alignment of the beam splitter with both of the photo-detectors seems to be the main reason to explain the previous plot. The picture below shows what is going on while cooling @ -100°C :

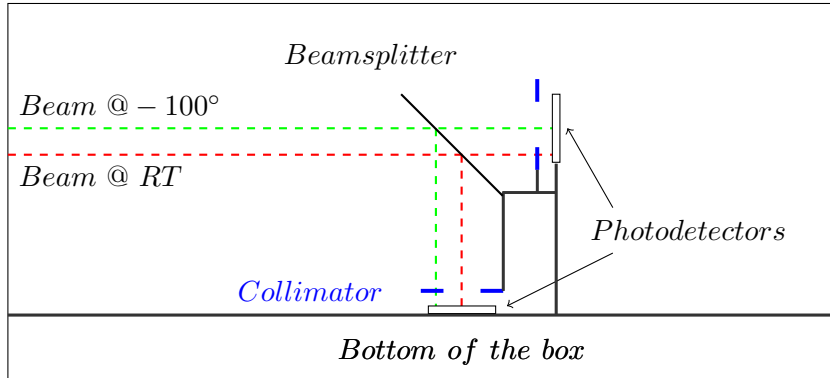


Figure 4.24: Effect of the temperature on the position of the two collimators.

The diameter of the hole of 1mm of each collimator is checked to be centered on the surface of each photo-detectors.

First a board holds both of the collimators, the beam splitter and the photo-detector on the top, as shown on figure 4.27. The photo-detector on the bottom can move independently of the previous board.

When the cooling system is working the temperature of the board decreases from 22°C to around 10°C ⁶ after 2 hours of running.

The opposite alignment of the beam with the photo-detector on the top and on the bottom explains the anti-correlation observed on figure 4.23 (top/bottom with cooling and with beam splitter).

Indeed we notice on 4.23 that the efficiency for the photo-detector on the top is lower on the beginning of the run (The board is at room temperature) than at the end (The temperature of the board is around 10°C). The efficiency for the photo-detector on the bottom acts in opposite way.

At room temperature (RT) the collimator (and so the photo-detector on the top since both are always centered) is not aligned with the beam of the Xenon flash lamp . On the contrary the collimator on the bottom is aligned with the beam. When the board is cooling down over the time, it moves a little bit. The consequence is that, at low temperature, the collimator on the top is aligned with the beam while the one on the bottom is no more aligned. This explains our previous results.

It is not only the beam splitter which moves over the time but all the board and so the collimator of the top and of the bottom. We could see that with run 2 (without beam splitter): we observe the same variation of efficiency for the photo-detector on the top (the efficiency of the photo-detector on the bottom is quiet null since no light can reach its area without beam splitter).

⁶Temperature of the box decreases from RT to around 15°C

Conclusion

The misalignment of the light explains our inconsistent results. A solution should be to focus the beam of the Xenon flash lamp on the collimator with a lens.

4.6 Dark Noise rate

4.6.1 Methodology for dark noise

One of the main source of noise limiting the SiPM performance is the dark noise rate, which mainly originates from electrons created thermally in the depletion region 4.10. These carriers trigger avalanches exactly as if pixels would have been fired by photons.

theoretical dark noise

To calculate the dark noise rate, the goal is to count the number of time the screen of the scope displays 1PE peak. A simple idea is to record the minimum of pulses in "the dark region"⁷. In the "light region" avalanches can be triggered by a photons or by hot carriers (dark noise) while in the dark region avalanches can be triggered only by hot carriers. But the probability of observing dark noise in the both regions is the same.

Here is the equation used to calculate the average number of dark noise $\langle DN \rangle$:

$$\langle DN \rangle = \ln \frac{N_{D0} + N_{L0}}{2 \cdot 15000}, \quad (4.8)$$

where N_{D0} and N_{L0} are the number of 0PE in the "dark and light region", respectively. 15000 waveforms are recorded for each region of $1000\mu\text{s}$. The total number of waveforms is $2 \cdot 15000 = 30000$ waveforms.

As described previously the dark noise rate follows a Poisson distribution:

$$P_{DN0} = e^{-\langle DN \rangle}, \quad (4.9)$$

where $\langle DN \rangle$ and P_{DN0} are the dark noise rate⁸ of and the probability of not observing any pulses in the dark region, respectively.

⁷See section 4.5

⁸The dark noise rate, in Hz, is the number of dark noise par second divided.

setting and algorithm

On the scope we trigger one the lamp and we record waveforms as described previously.

The C++ code "fillNtp.exe" smooths a waveform (to decrease the Gaussian noise and increase the ratio Signal/Noise), set two windows of $1\mu\text{s}$ each in the "light and dark region" and records the minimum of a waveform and plot an histogram.

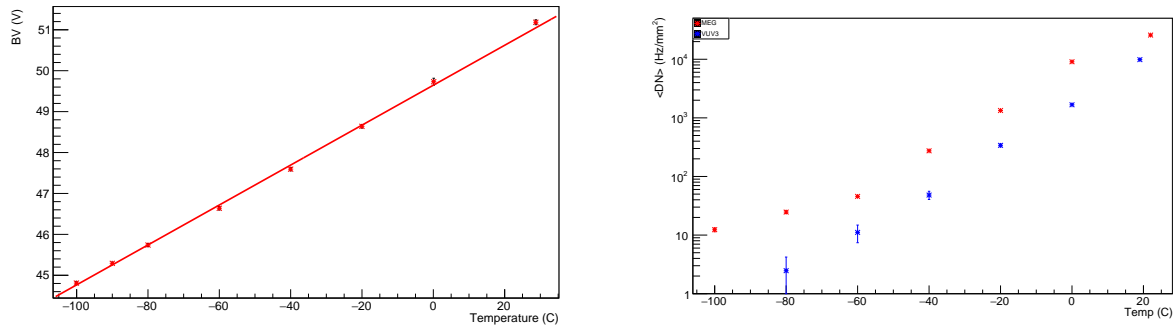
Here is an example of line command: `bin/fillNtp.exe -r 956 -s 10 -w 1000 -b 1500 -a 8500`, with "-r, -s, -b, -a" are described above.

4.6.2 Results

The histogram looks the same than the one of the previous section 4.5.

The first goal is to plot the dark noise rate versus temperature. Moreover the over-voltage for each temperature must be the same since the over-voltage applied on the photo-detector changes pulse shapes. The appendix C explains how we proceed to calculate the breakdown voltage for the VUV3 SiPM.

We worked with low over-voltage to avoid crosstalk and the previous histograms allow plotting the dark noise rate $\langle DN \rangle$ versus temperature since the dark noise depends of the temperature 4.3.4:



(a) The fitting allows finding a breakdown voltage of 44.73V for the VUV3 SiPM at -100°C .

(b) Dark noise rate versus temperature for the **VUV3 SiPM** and the **MEG MPPC**.

Figure 4.25: The breakdown voltage allows working on the same OV for different temperature and thus to plot DN versus temperature.

Also as the VUV3 SiPM from HAMMAMATSU seems to be interesting fro nEXO, it is also interesting to plot dark noise rate versus over-voltage at -100°C . This plot will be compared with the one showing correlated avalanche versus over-voltage at the same temperature for the VUV3.

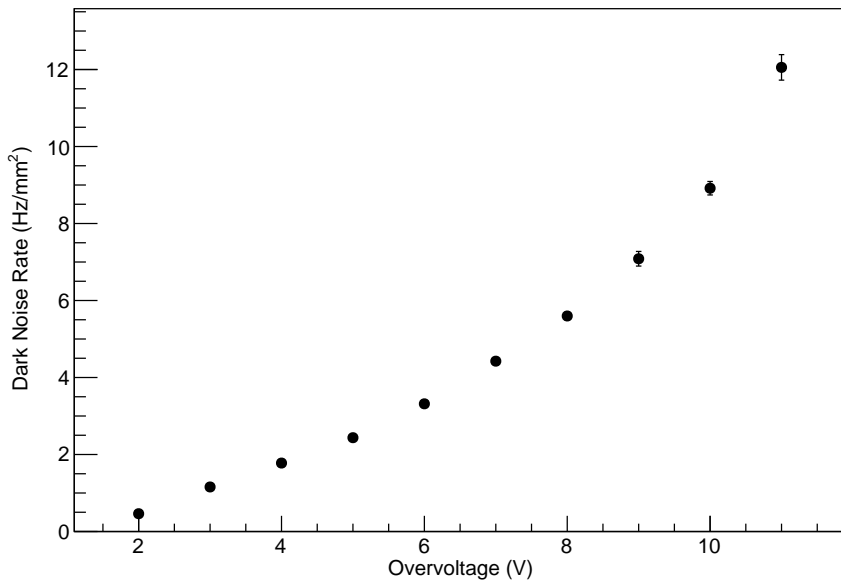


Figure 4.26: Dark noise rate increases with the over-voltage applied on the VUV3 SiPM at -100°C .

4.6.3 Analysis: Poisson distribution

The figure 4.25(b) shows clearly that the dark noise $\langle DN \rangle$ rate follows a Poisson distribution. The dark noise depends on the temperature: when the temperature increases the number of pulses triggered by hot carriers increases and so the probability of not observing any pulses in the dark region decreases. That means that for a same total number of waveforms, the 0PE peak of the histogram 4.21 decrease while the other peaks (1PE, 2PE peaks ...) increases.

Also the figure 4.26 shows that the dark noise dependence on over-voltage is found to be linear up to 7 over-voltage. This observation is consistent with previous results shown by nEXO [13].

4.6.4 conclusion

Compared to the MEG MPPC, the VUV3 SiPM is a good candidate for nEXO. Moreover up to 13 over-voltage 4.26 the dark noise rate for such a device is still bellow 50 Hz/mm².

4.7 Correlated avalanches: CT and AP

Correlated avalanches refer to crosstalk 4.3.4 and after pulse 4.3.4.

4.7.1 Methodology

Crosstalk

When we trigger on the lamp, histograms from the dark region show the 0PE peak ,1 PE peak, 2PE peak ... where the 0PE peak doesn't count any pulses, the 1PE peak counts single pixel avalanches, the 2PE peak counts pulse shapes triggered from two different pixels ...

When we trigger on the photo-detector, histograms shows the same thing but the previous 0PE peak counts single pixel avalanches (and triggered by hot carriers) while the previous "1PE peak" counts pulse shapes triggered from two different pixels ...

The second method is more simple than the first one because we know for sure there will always be a pulse shape since the oscilloscope records a waveform if the signal reaches a certain threshold (6 mV/div) below the Gaussian noise.

Moreover we managed to make appear each waveform on the middle of the oscilloscope.

The average number of crosstalk $\langle CT \rangle$ could be calculated assuming that:

$$\langle CT \rangle = -\ln\left(\frac{N_{1PE}}{N_{>1PE}}\right), \quad (4.10)$$

where N_{1PE} matches with the 1PE peak of the previous histogram and $N_{>1PE}$ is calculated by integrating that whole histogram from the beginning of the 1PE peak.

When the over-voltage increases, the 1PE peak decreases while all other peaks increase.

After triggering on the photo-detector, a C++ code "fillNtp.exe" smooths a waveform, sets a window size of 200ns (100ns before and 100ns after) on the middle of a waveform ⁹ and records the minimum of that waveform in a histogram.

Here is an example of line command: `bin/fillNtp.exe -r 1605 -s 10 -w 200 -b 4900`, with "-r, -s, -b" are described in section 4.5.

Afterpulse

A C++ code called "pulsefinding.exe" finds after pulses. This reference [10] from TRIUMF gives some explanations and results.

A certain number of waveforms (15000 in that case) is recorded. The amplitude and the time of the first pulse shape of the first waveform (among 15000) are recorded. Then the amplitude and the time of each pulse shape for all the waveform are recorded. Pulse shapes could match with pulse shapes from crosstalk 4.3.4, or from dark noise 4.3.4 or from after pulses 4.3.4.

In the last case, it is quiet difficult to identify after pulses since they can appear at least 10ns after a primary peak 4.13 (A primary peak generates after pulses). To discriminate after pulses

⁹The middle is 5μs since each waveform lasts 10μs.

from Gaussian noise a common solution is to fit each pulse as describe in that paper [10]. The drawback of fitting a waveform is the time of operating such code.

The C++ code called "pulsfinding.exe" do not fit a waveform since pulse shapes from VUV3 SiPM or from MPPC MEG since they are quiet recognizable (large fall time).

Here is the algorithm of that code:

- Scan a waveform
- Calculate the standard deviation of the baseline and set a threshold at 4.5 baseline,
- Find a primary peak and record time ($Time_{max}$) and absolute amplitude (Amp_{max}),
- Find all local maxima around a primary peak, time ($Time_{max}$) and absolute amplitude (Amp_{max}),
- Check 6 ns before and 1 ns after a local maximum,
- Record time ($Time_{ap}$) and relative amplitude (Amp_{ap}) from that local maximum,
- Calculate the ratio R to discriminate after pulse from Gaussian noise fluctuation:

$$R = \frac{Amp_{ap}}{Amp_{max}} * \ln(Time_{max} - Time_{ap}) \quad (4.11)$$

- Record time and absolute amplitude of that local maximum.

The picture below will complete the previous explanation:

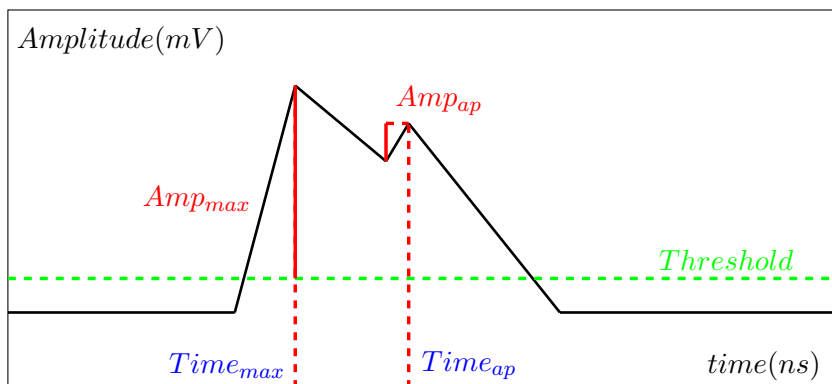


Figure 4.27: The shematic algorithm to find after pulses.Pulse shapes are set positive.

Also we would like to remind that the probability of not observing after pulses (P_{0AP}) follows a Poisson distribution :

$$P_{0AP} = e^{-<AP>} , \quad (4.12)$$

where $<AP>$ is the average number of after pulses.

4.7.2 Results

Here is an example of an histogram used for crosstalk. From right to left 1PE, 2EP, 3PE, 4PE, 5PE:

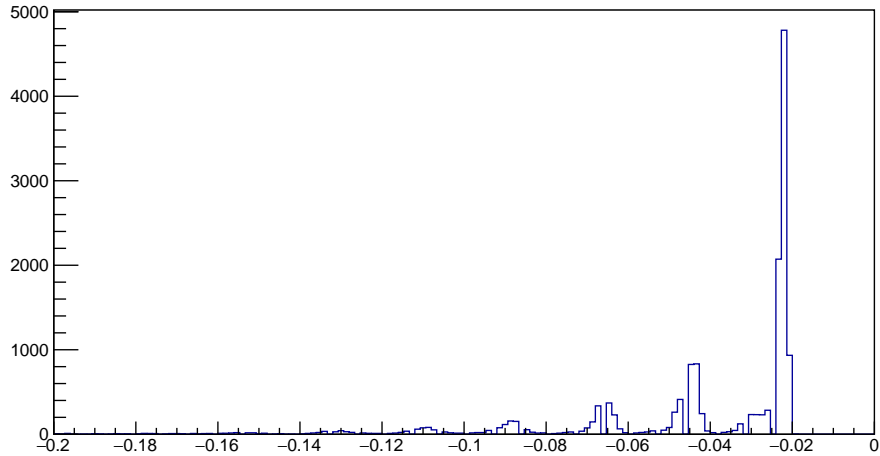


Figure 4.28: An histogram from crosstalk analysis. The device is a VUV3 SiPM at -100°C at 5 over-voltage.

Crosstalk from different devices (coated SiPM, MEG MPPC and VUV3 SiPM) are plotting on the figure below.

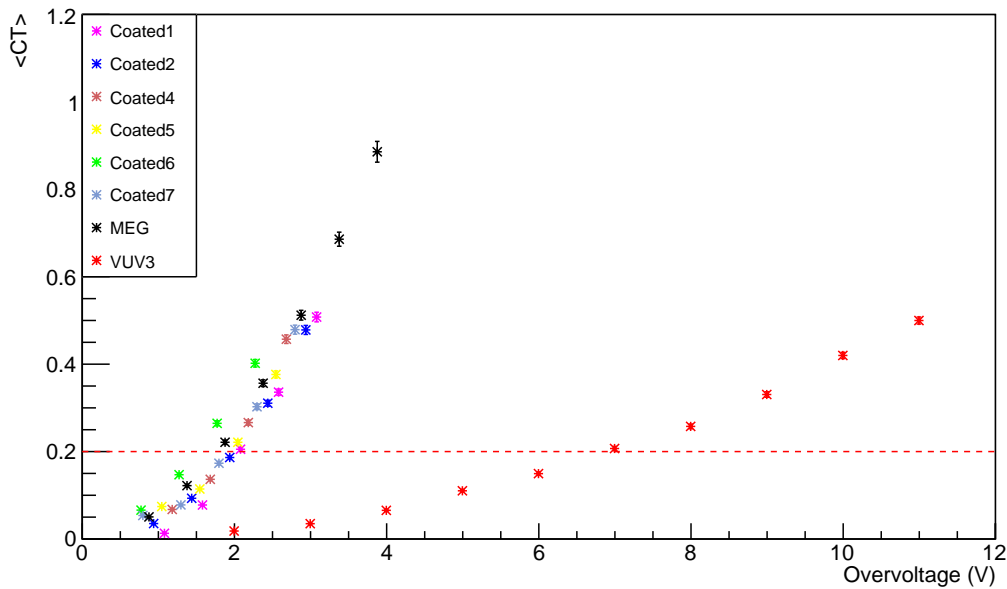
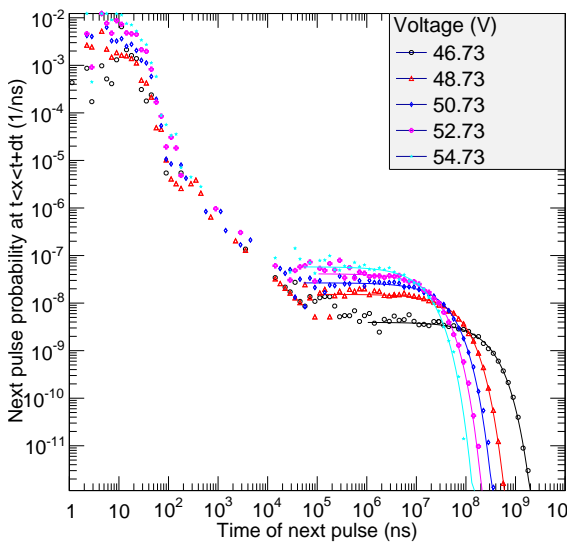
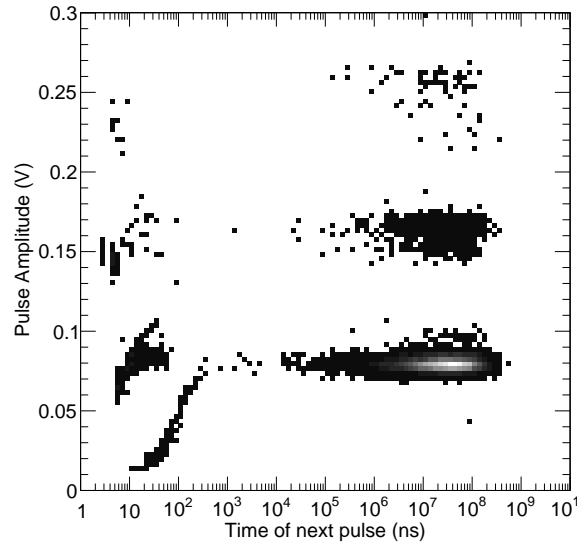


Figure 4.29: Crosstalk for the VUV3 SiPM reminds below 2 up 6.5 OV.

The pulsefinding.exe function allows plotting two different graphs. The first one shows the next pulse probability versus time for different over-voltages for the VUV3 SiPM at -100°C while the second plot shows the pulse amplitude versus time for the same device at 5 over-voltage at the same temperature:



(a) Probability of observing next pulses after the first one of the first recorded waveform. Two tails separated at $50\mu\text{s}$ are quite visible.



(b) Amplitude of pulses versus time for the VUV3 SiPM.

Figure 4.30: Those two plots are the unique signature of a photo-detector.

Moreover combining two different methods -fitting and counting- allows plotting the average number of after pulses ($\langle AP \rangle$) versus over-voltage:

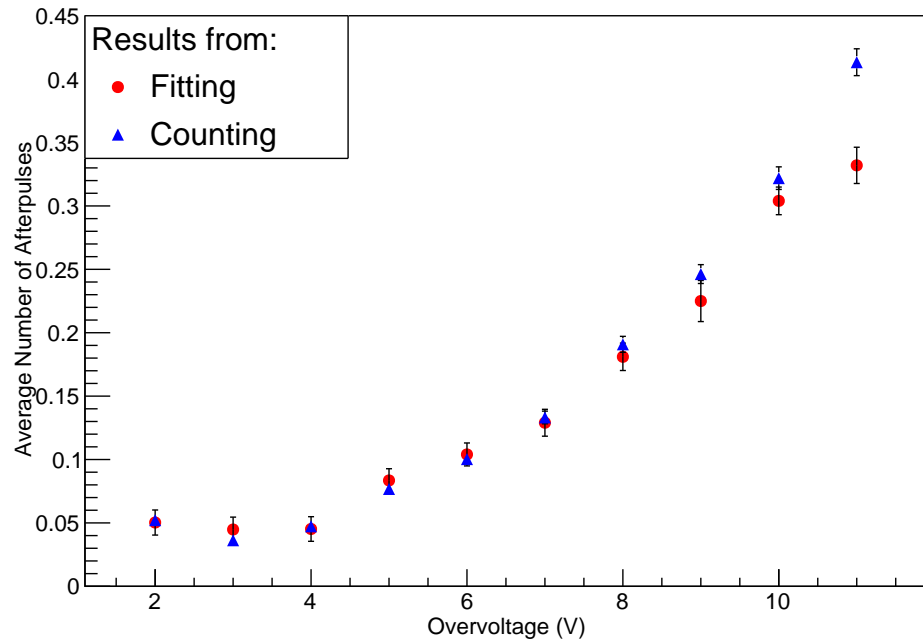


Figure 4.31: Average Number of after pulses for the VUV3 SiPM at -100°C .

At least adding results from the figure 4.29 and from the last figure 4.31 allows plotting the average number of correlated avalanches ($\langle CT \rangle + \langle AP \rangle$) versus over-voltage:

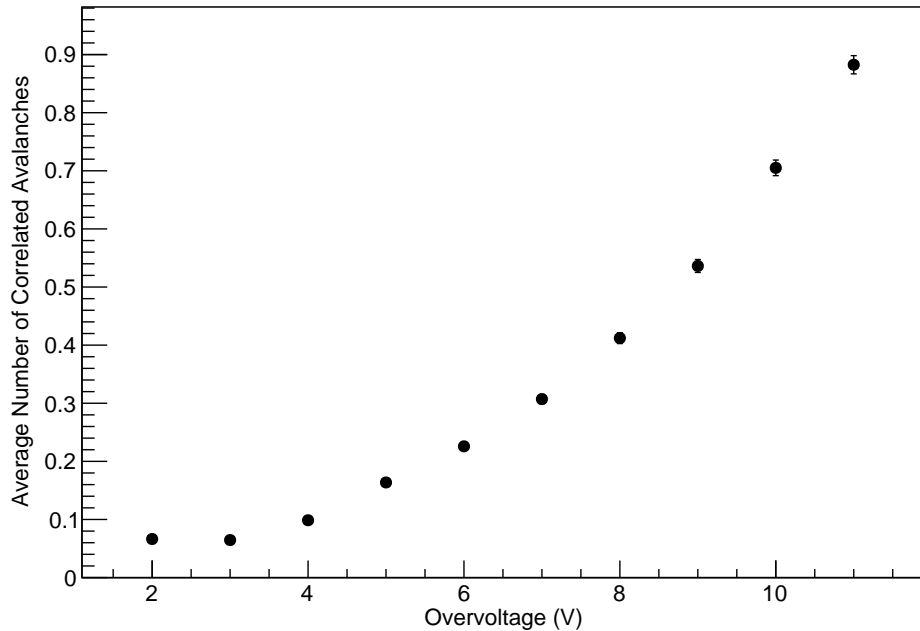


Figure 4.32: Average Number of Correlated Avalanches for the VUV3 SiPM at -100°C .

4.7.3 Analysis

Crosstalk

CT depends mainly of the over-voltage applied on the photo-detector.

When we increased the voltage applied on the photo-detector, pulse shapes increases. So the number of 2PE peak of the previous histogram increase while the number of 0PE peak decreases for a same number of waveform and thus, the crosstalk increases according the previous relation 4.10.

Moreover the crosstalk for the VUV3 SiPM is very interesting because the average number of crosstalk ($\langle CT \rangle$) reminds below 0.2 per parent pulse.

After Pulses

The two previous plots side by side 4.30 are quiet interesting since they characterize a VUV3 SiPM.

The distribution of the timing difference between consecutive pulses 4.30(a) is used to measure the after pulses and the dark noise rates.

For measuring after-pulsing rate, the starting pulses are required to correspond to the oscilloscope trigger in order to properly account for the oscilloscope dead time. The starting pulses are

also required to correspond to single pixel avalanches (i.e. triggers with cross-talk are excluded) in order to measure the after-pulsing rate generated by a single parent avalanche. On the other hand, the second pulse can have any amplitude (above the noise).

The figure 4.30(a) shows clearly the oscilloscope dead time ¹⁰ because of a sort of cut at $50\mu s$ (whatever is the voltage) which separates two different tails.

That reference from nEXO [10] (page 7, equation 1 and 4) helps us to fit the tail after $50\mu s$. Here is the equation used:

$$P_{total} = P_{0AP} \cdot <DN> \cdot e^{-<DN>\cdot t}, \quad (4.13)$$

where P_{0AP} , $<DN>$ and t are the probability of observing no after pulse, the dark noise rate (Hz/mm^2) and the time, respectively.

Then P_{0AP} is extracted from that fitting and assuming that the after pulse follows a Poisson distribution 4.12, it is possible to calculate the average number of after pulses ($<AP>$) for different voltages. That fitting method shows clearly the $<AP>$ versus over-voltage for the VUV3 SiPM at -100°C .

Also an algorithm let us count the average number of after pulses. Indeed a ratio is defined :

$$R = \frac{\text{number of after pulses}}{\text{number of primary peaks}}, \quad (4.14)$$

where the number of primary peaks corresponds to all peaks which are not counting as after pulses since they trigger after pulses.

If the time between two consecutive pulses $-\Delta t-$ is lower than $50\mu s$ and upper than $10\mu s$, pulses are considered as after pulses. If that Δt is lower than $10\mu s$ and if the amplitude of founded pulses are upper than 0.5 PE (to avoid Gaussian noise fluctuation), those pulses are crosstalk. Else, all other pulses are counting as after pulses.

The two methods -fitting and counting - match quiet well as we can see it on the figure 4.31.

For measuring the dark noise, the method is to fit the tail after $50\mu s$ since pulses after $50\mu s$ are considered as pulses triggered by hot carriers. We noticed that after pulses should be generated in a lapse of time before $50\mu s$ and thus, pulses after $50\mu s$ can be counted as dark noise.

As well as the number $<AP>$ is deduced from the fitting 4.13, the dark noise rate $<DN>$ is deduced from the fitting. The figure 4.30(a) shows clearly that the dark noise rate depends of the voltage applied on the VUV SiPM (breakdown voltage of $44.73\text{V} +/- 0.03$ at -100°C) and allow also plotting the previous figure 4.26.

For the distribution of the pulse amplitude versus time, there is no correlation between time and amplitude except below $3\mu s$ which is the recovery time of a pixel. The recovery time is the amount of time before pulses will be release with their full amplitude.

Physically inside the photo-detector, after an avalanche, the voltage across the diode recovers with a time constant given by the product of the pixel capacitance and quenching resistance. Pulses with high amplitude must come from different pixels (crosstalk) even though they occurred within the recovery time scale. If so the quenching resistor absorbs the created carriers and pulses do not have enough time to release with their full amplitude.

¹⁰The dead time appears when the oscilloscope is busy to do something else than triggering

The main band at 80 mV corresponds to pulses from single pixel avalanches while the other bands corresponds with pulses whose amplitude is two or three or more time larger pulse amplitude from the main band.

Correlated Avalanche

The last figure 4.32 shows the correlated avalanches of the VUV3 SiPM at -100°C . Adding the figure 4.31 and the figure 4.29 allows plotting that last figure since the average number of correlated avalanches is the sum of the average number of crosstalk and the average number of after pulses.

The VUV3 SiPM lets us increase the over-voltage up to 5V and the average number of correlated avalanches is still under 0.2 per parent pulse. That means that below 5 over-voltage, the probability of observing correlated avalanche generated by a primary pulse is below 20% 3.1.3.

Chapter 5

Synthesis

One of the main goal of this internship was to calculate the efficiency for different photo-detectors (MEG MPPC, SiPM, coated SiPM, FBK ...).

Nevertheless we noticed that our results for the VUV3 SiPM are not reproducible. In order to understand what is(are) the source(s) of that non reproducibility, we tried to eliminating different parameters such as the position and the voltage of the lamp, the quantity of oxygen inside the box and some dust on the sensitive area of the photo-detectors.

We arrived at the conclusion that the misalignment of the narrow beam with the collimator on the top and on the bottom may be the main source of our problem.

Moreover working at -100°C seems to influence the position of the board holding the two collimators, the beam splitter and the photo-detector on the top: after three hours of cooling, the efficiency of the photo-detector on the top increases while the efficiency of the one on the bottom decreases. Nevertheless both of them seems to reach a sort of plateau which allow making a temporary comparison between the MEG MPPC and the VUV3 SiPM at -100°C (assuming that the beam remains constant).

Recommendations We recommend to the next students to enlarge the beam with a divergent lens. So that the beam could always reach the hole of 1 mm of the collimator even though the board is moving down while cooling at very low temperature.

On the contrary results about dark noise and correlated avalanches are confident, especially for the VUV3 SiPM which fulfills the last two requirements for nEXO:

- Its dark noise rate is less than 3 Hz/mm^2 for an over-voltage of 5V at -100°C ¹.
- Its average number of correlated avalanches is less than 0.2 per parent pulses for the same over-voltage at the same working temperature².

Recommendations We also recommend to the next students to confirm such results for the MEG MPPC and the coated SiPM B.2.

At least some investigations need to be done about the attenuation of light as described in appendix C.

¹It is required 50 Hz/mm^2 for such a temperature.

²It is required 0.2 per parent pulses in the same conditions.

Chapter 6

Professional assessments

This internship has been very beneficial and I found it very interesting. I learned a lot from my co-workers about SiPMs. Their knowledges on such a subject let me improve my scientific and rigorous thinking in physics. I have always solicited them when I was fighting with some difficulties.

I was happy to use my theoretical knowledges about electronics, matter physics and physics about detectors. I also improved my engineering thinking by trying to adopt practical solutions for all issues we had.

Chapter 7

Human impact

I really enjoyed working at TRIUMF and also working in an English environment. From the beginning of my internship I tried to improve my English skills in oder to improve my knowledges on the subject. The natural open minding of the Canadian help me for that.

I also enjoyed working in a laboratory on a research internship. Having good and new results, with a possible publication at the end, was one of my motivations at work. I also enjoyed working on that internship with a difficulty linked to a research subject.

I also enjoyed working with autonomous and flexible hours.

I enjoyed that internship because I was asked to use my theoretical knowledges to explain physical phenomena.

Chapter 8

Conclusion

This internship ends my engineering study at Télécom Physique Strasbourg . This has been a very good experience which allow taking responsibilities in nEXO's collaboration.

My internship was a very interesting technological subject. I have been asked to use the two different parts of my engineering and scientific courses I could also discover working in a team for a hug collaboration.

As far as possible my work contributed to make some progress on the study of SiPMs. Results are quiet positive and put forward my engineering formation.

Bibliography

- [1] Mark Thomson, *Modern Particle Physics*, Hardcover, **Oct 21, 2013**.
- [2] Frederick Reif, *Fundamentals of Statistical and Thermal Physics*, Hardcover, **Jan 6, 2009**.
- [3] https://en.wikipedia.org/wiki/Majorana_fermion.
- [4] *Scintillation light detection in nEXO*, **May 13, 2015**.
- [5] http://www.hamamatsu.com/us/en/community/optical_sensors/tutorials/physics_of_mppc/index.html?utm_source=googleplus&utm_medium=social&utm_campaign=hc-social.
- [6] www.hamamatsu.com/resources/pdf/etd/Xe-F_TLS1003E.pdf, page 4, Flash Pulse Waveform.
- [7] https://en.wikipedia.org/wiki/P%26E2%2880%29n_junction.
- [8] Kenneth R. Spring and Michael W. Davidson, *Avalanche Photodiodes*, available at <http://hamamatsu.magnet.fsu.edu/articles/avalanche.html>.
- [9] *MPPC and MPPCC module for precision measurements*, HAMMAMATSU, **May 13, 2015**, page 2, figure 2.
- [10] I. Ostrovskiy et al., *Characterization of Silicon Photomultipliers for nEXO*, arXiv:1502.07837v2 [physics.ins-det], **Jul 6, 2015**
- [11] Patrick Eckert et al., *Characterisation studies of silicon photomultipliers*, available at <http://arxiv.org/abs/1003.6071>, **2010**.
- [12] <http://www.teo.com.cn/filespath/files/20130802133536.pdf>, page 4, figure Phelham Research Opticall L.L.C Narrowband Filter P/N:172-NB Filter.
- [13] Pierre-Andr'e Amaudruz et al., *Pixelated Geiger-Mode Avalanche Photo-Diode Characterization through Dark Current Measurement*, arXiv:1312.0545 [physics.ins-det], **Dec 2, 2013**.

Appendix A

Terminology

Acronym	Meaning
EXO	Enriched Xenon Observatory
nEXO	next generation Enriched Xenon Observatory
SiPM	Silicium Photo Multiplier
MPPC	Multi-Pixel Photon Counter
VUV	Ultra Vacuum
APD	Avalanche Photo-diode
BV	Breakdown Voltage
OV	Over Voltage
DN	Dark Noise
CT	Crosstalk
PE	Photon Electron

Appendix B

Details about the setup

B.1 Pictures of the setup

Here is a general picture of the setup. The table below the figure explains the number.



Figure B.1: General pictures of the setup.

Here is the meaning of each number:

Numbers	Meaning
1	Set the voltage to the lamp
2	Set the voltage of 12 V for both amplifiers
3	Set volatge of 5 V to control device number 4,5,6 from a computer
4	Set voltage of the photodetector on the bottom
5	Set voltage of the photodetector on the top
6	Display and Record temperature from all sensors
7	Set the trigger of the lamp
8	Set the voltage for a PMT
9	Set temperature to cool down the photodetector on the bottom
10	Allow cooling down
11	Small bottle whose N2 is used to cool down the photodetector
12	Big bottle to fille the box with N2
13	Oscilloscope allowing displaying and registering waveforms

Figure B.2: Different devices used for the setup.

To reduce light leaks from the Xenon flash lamp , a black box covers the lamp:



Figure B.3: A black box covering the lamp blocks light leaks from it.

Then to absorbe radio frequency leaks from the lamp, 2 pieces of metal are added on the top of that box:



Figure B.4: Pieces of metal seem to absorbe radio frequency leaks from the lamp.

A photodetector on the bottom can be centered with the hole of 1 mm of the collimator with the help of 2 lines:

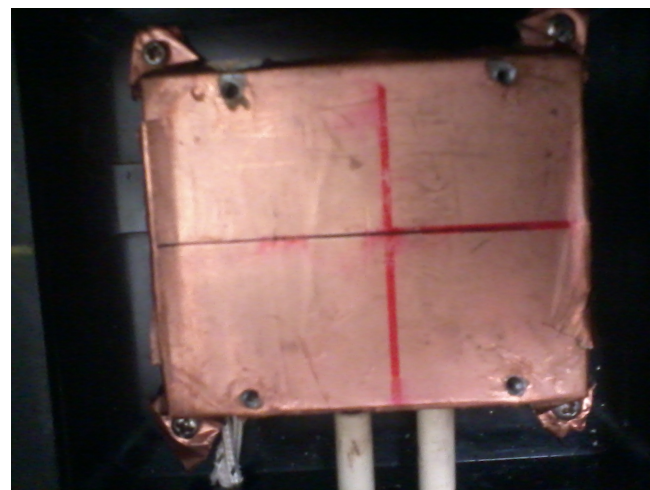


Figure B.5: These two lines on the shock guide to center the photodetector with the hole of 1 mm of the collimator.

A solution to align properly the photodetector on the top with the hole of 1 mm of the collimator:



Figure B.6: It is quiet difficult to align properly the photodetector of the top with a hole of 1 mm.

B.2 Details about waveforms

The voltage applied on the lamp makes moves the time of apparition of pulses triggered by photons:

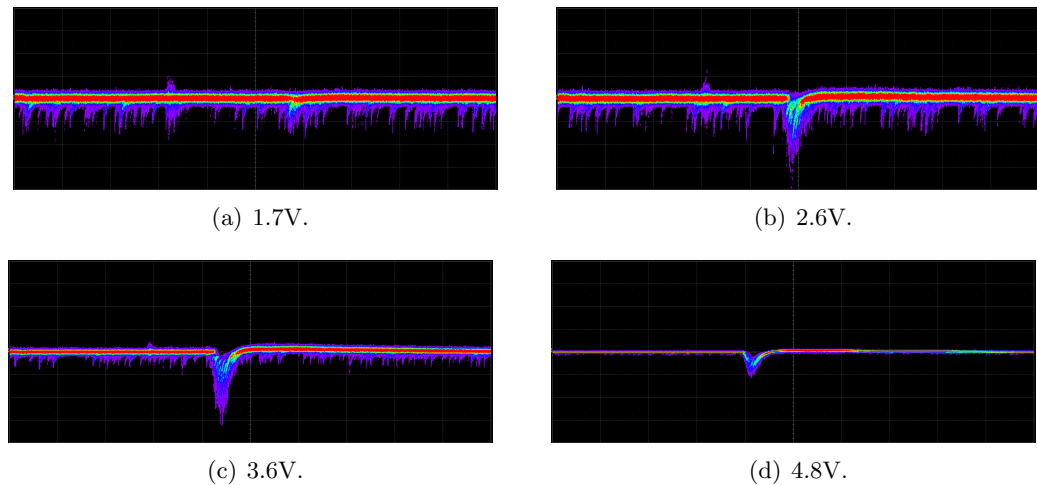


Figure B.7: Increasing the voltage makes appear earlier pulses triggered by photons.

To increase the signal from the photo-detectors, two amplifiers are used:



Figure B.8: Signals from each photo-detector are increased by using amplifiers.

Difference between photon saturation and electronic saturation:

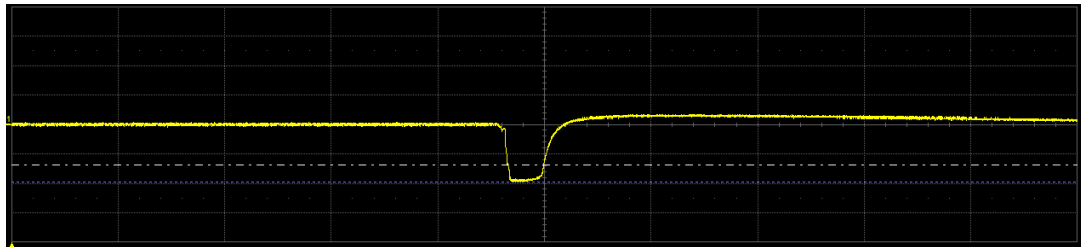


Figure B.9: Electronic saturation from the MEG MPPC. Horizontal axis is $1\mu\text{s}/\text{div}$ and Vertical axis is $1\text{V}/\text{div}$.

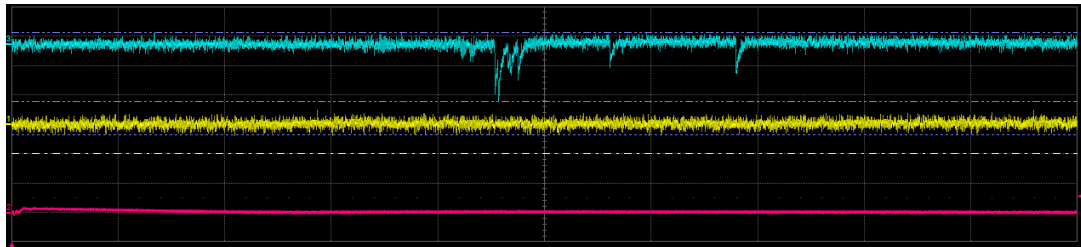


Figure B.10: The blue signal shows photon saturation: too many peaks in the $1.4\mu\text{s}$ region. Horizontal axis is $1\mu\text{s}/\text{div}$ and Vertical axis is $10\text{mV}/\text{div}$.

Appendix C

Tests

C.1 Attenuation of light

The optical corporation -Pelham Research Optical LLC - shows in the figure below the coefficient of transmission of the filters used for our setup:

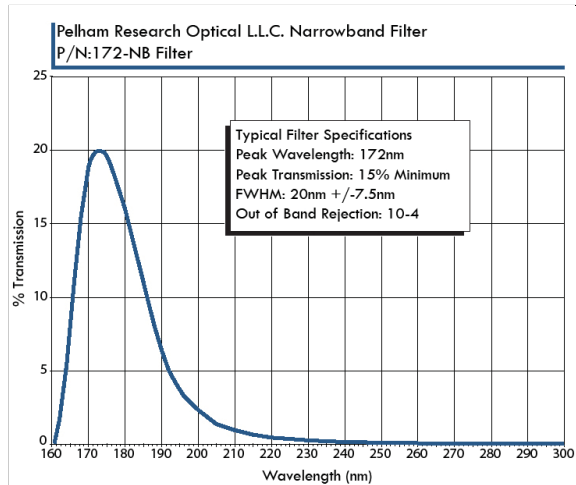


Figure C.1: The coefficient of transmission for our filters is less than 20% according to the manufacturer [12].

To check that coefficient we calculated the efficiency of a photo-detector on the bottom (VUV2 SiPM), in the same experimental conditions. For the first run, the filter was in front of the surface of that photo-detector and for next run, we removed that filter. Then we divided the second result for the efficiency by the first one. That ratio gave us : 18.79%.

Our results are in the file "*Test_ratiofilter20%.ods*" on GitHub.

C.2 Calibration of temperature sensors

To calibrate the different temperature sensors used for our setup, we attached each of them on the cooling shock.

Then we set different temperature thanks to the device which allow reaching very low temperature.

Then we recorded each temperature ¹ displays by each of temperature sensors and we obtained one of these figures below:

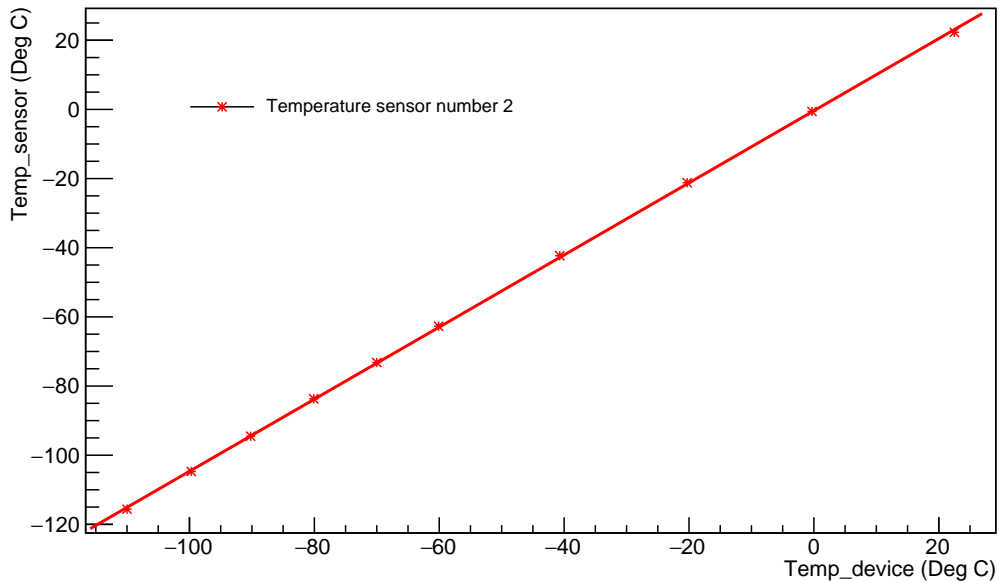


Figure C.2: Temperature of one of the sensors versus temperature displays by the cooling system.

Taking as reference the temperature displays by the cooling system, after fitting the previous shape, it is now possible to correct each temperature of our sensor, since the equation of the previous fitting is:

$$Temp_{sensor} = p_0 + p_1 \cdot Temp_{device}, \quad (C.1)$$

with

$$p_0 = -0.379691 + / - 0.233424 \quad (C.2)$$

and

$$p_1 = 1.04282 + / - 0.0033805. \quad (C.3)$$

¹Here is the different temperatures: 22.3°C, -0.3°C, -20.3°C, -40.7°C, -60.1°C, -70°C, -80.1°C, -90.2°C, -99.7°C, -110°C

C.3 Breakdown voltage calculation

To plot the figure showing the breakdown voltage for the VUV3 SiPM versus temperature 4.25(a), here is the method we used to calculate the breakdown voltage of the VUV3 SiPM for different temperatures.

After setting the desired temperature and triggering on the photo-detector, we took 10 points matching with different voltages and we saved 300 waveforms. It was not useful to record more waveforms since the error bars are quiet small (which is not the case for the MEG MPPC).

Then the C++ code called "Normgain.exe" is used to calculate the gain at of the device for the different applied voltages. As the temperature has an influence on the gain, we tried to record all the waveforms at the same temperature ² for such voltages. That is why we registered only 300 waveforms.

Then we plotted the calculated gain versus the applied voltages for a desired temperature:

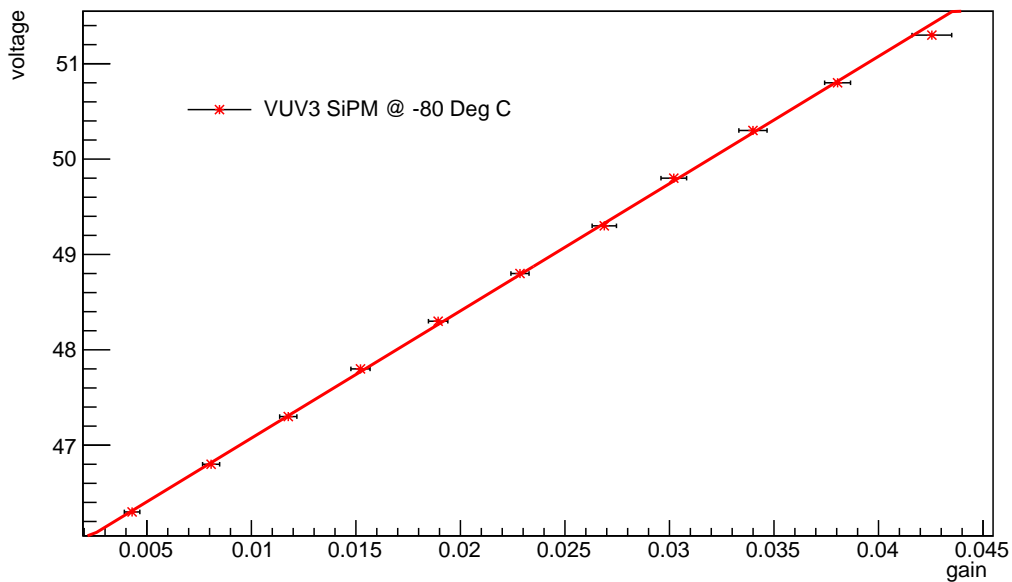


Figure C.3: At -80° this figure -gain versus voltage- allow determinate the breakdown voltage thanks to the fitting.

Here is the two parameters obtained from that fitting:

$$p0 = 4.57394e + 01 \pm 3.83652e - 02, p1 = 1.33438e + 02 \pm 1.83935e + 00 \quad (\text{C.4})$$

²A variation of temperature of 0.2° is admissible.

C.4 Error bars calculation

Here is the error bars calculation

C.4.1 PE

Here is the equation used to calculate the average number of photon electrons $\langle PE \rangle$:

$$\langle PE \rangle = -\ln\left(\frac{P_{L0}}{P_{D0}}\right), \quad (\text{C.5})$$

where $\langle PE \rangle$, P_{L0} and P_{D0} are the average number of photon electron, the probability of not observing any pulses in the “light region” and in the “dark region”, respectively.

Then assuming that the total number of recorded waveforms is $N_{tot} = 15000$:

$$\sigma_{P_{L0}} = \sqrt{\frac{P_{L0} \cdot (1 - P_{L0})}{N_{tot}}} \quad (\text{C.6})$$

and

$$\sigma_{P_{D0}} = \sqrt{\frac{P_{D0} \cdot (1 - P_{D0})}{N_{tot}}} \quad (\text{C.7})$$

So here is the error bar for the $\langle PE \rangle$:

$$\sigma_{\langle PE \rangle} = \sqrt{\left(\frac{\Sigma_{P_{L0}}}{P_{L0}}\right)^2 + \left(\frac{\Sigma_{P_{D0}}}{P_{D0}}\right)^2} / N_{tot} \quad (\text{C.8})$$

C.5 DN

Here is the equation used to calculate the average number of dark noise $\langle DN \rangle$:

$$\langle DN \rangle = \ln \frac{N_{D0} + N_{L0}}{2 \cdot 15000}, \quad (\text{C.9})$$

Lets set:

$$N_{DN0} = N_{D0} + N_{L0}, \quad (\text{C.10})$$

Thus:

$$P_{DN0} = \frac{N_{DN0}}{2 \cdot N_{tot}} \quad (\text{C.11})$$

And:

$$\sigma_{P_{DN0}} = \sqrt{\frac{P_{DN0} \cdot (1 - P_{DN0})}{2 \cdot N_{tot}}} \quad (\text{C.12})$$

So here is the error for the $\langle DN \rangle$:

$$\sigma_{\langle DN \rangle} = \frac{\sigma_{P_{DN0}}}{P_{DN0}}. \quad (\text{C.13})$$

C.6 CT

Here is the equation used to calculate the average number of crosstalk $\langle CT \rangle$:

$$\langle CT \rangle = -\ln\left(\frac{N_{1PE}}{N_{>1PE}}\right), \quad (\text{C.14})$$

Thus:

$$P_{1PE} = \frac{N_{1PE}}{N_{>1PE}}, \quad (\text{C.15})$$

Thus:

$$\sigma_{P_{1PE}} = \sqrt{\frac{P_{1PE} \cdot (1 - P_{1PE})}{N_{>1PE}}} \quad (\text{C.16})$$

So here is the error for the $\langle CT \rangle$:

$$\sigma_{\langle CT \rangle} = \frac{\sigma_{P_{1PE}}}{P_{1PE}}. \quad (\text{C.17})$$

C.7 Test to check light leaks

To check if we could observe some light leaks from outside of the box, we did a 3 consecutive runs:

- Run 1: Lights of the room are off and a black tissue covers the box(black circle),
- Run 2: Lights of the room are on and a black tissue covers the box(red triangle),
- Run 3: Lights of the room are on and a black tissue is moved from the box (blue lossgage).

Plotting next pulses versus time for the same device at the same over-voltage shows clearly light leaks from outside of the box. Indeed the blue lossage doesn't match at all with the first two runs.

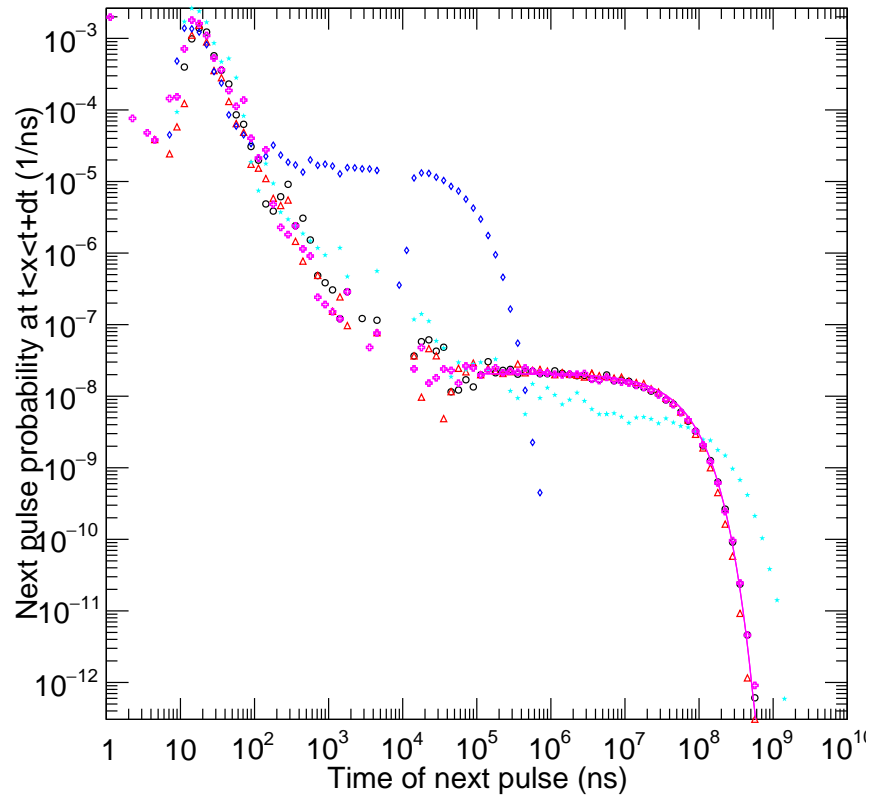


Figure C.4: Light leaks from outside of the box.